

# Accuracy of DLPNO–CCSD(T) Method for Noncovalent Bond Dissociation Enthalpies from Coinage Metal Cation Complexes

Yury Minenkov, Edrisse Chermak, and Luigi Cavallo\*

KAUST Catalysis Center (KCC), King Abdullah University of Science and Technology, Thuwal-23955-6900, Saudi Arabia

## S Supporting Information

**ABSTRACT:** The performance of the domain based local pair-natural orbital coupled-cluster (DLPNO–CCSD(T)) method has been tested to reproduce the experimental gas phase ligand dissociation enthalpy in a series of  $\text{Cu}^+$ ,  $\text{Ag}^+$ , and  $\text{Au}^+$  complexes. For 33  $\text{Cu}^+$ –noncovalent ligand dissociation enthalpies, all-electron calculations with the same method result in MUE below 2.2 kcal/mol, although a MSE of 1.4 kcal/mol indicates systematic underestimation of the experimental values. Inclusion of scalar relativistic effects for Cu either via effective core potential (ECP) or Douglass–Kroll–Hess Hamiltonian, reduces the MUE below 1.7 kcal/mol and the MSE to  $-1.0$  kcal/mol. For 24  $\text{Ag}^+$ –noncovalent ligand dissociation enthalpies, the DLPNO–CCSD(T) method results in a mean unsigned error (MUE) below 2.1 kcal/mol and vanishing mean signed error (MSE). For 15  $\text{Au}^+$ –noncovalent ligand dissociation enthalpies, the DLPNO–CCSD(T) methods provides larger MUE and MSE, equal to 3.2 and 1.7 kcal/mol, which might be related to poor precision of the experimental measurements. Overall, for the combined data set of 72 coinage metal ion complexes, DLPNO–CCSD(T) results in a MUE below 2.2 kcal/mol and an almost vanishing MSE. As for a comparison with computationally cheaper density functional theory (DFT) methods, the routinely used M06 functional results in MUE and MSE equal to 3.6 and  $-1.7$  kcal/mol. Results converge already at CC-PVTZ quality basis set, making highly accurate DLPNO–CCSD(T) estimates affordable for routine calculations (single-point) on large transition metal complexes of  $>100$  atoms.



## 1. INTRODUCTION

Computational chemistry is routinely applied nowadays to support and integrate experimental studies in transition-metal catalysis.<sup>1–7</sup> The successful standalone experimental-free theoretical predictions in this field are far less common, however.<sup>8</sup> While some failures in theoretical predictions are originated from the complexity of the systems themselves and can be ameliorated by proper inclusion of the effects deriving from incomplete sampling of the conformational space and/or solvation,<sup>1,9</sup> the other failures are related to the accuracy of electronic structure methods. In general, scalar/vector relativistic effects, basis set completeness and multireference character of some systems should be properly addressed regardless on the electronic structure method used.<sup>10,11</sup> When it comes specifically to density functional theory (DFT) methods, which is the only affordable computational protocol to study systems of “realistic-size”, one has to remember that the performance of the underlying exchange–correlation (XC) functionals is not uniform, and provides low to high accuracy predictions depending on the chemical system under study.<sup>12</sup> The careful “calibration” against highly accurate experimental measurements or wave function theory (WFT) calculations helps to improve upon the situation as well as latest developments in functional design.<sup>9,13–27</sup> However, the question to what extent the chemical system under study is different from the ones used for calibration of a given functional and, more important, the amount of highly accurate experimental measurements is limited.

On the other hand, so-called ab initio WFT methods<sup>28</sup> are rigorous and allow to systematically achieve chemical accuracy without any calibration against experimental data. In particular, the coupled cluster approximation with inclusion of doubles and triples excitations (CCSD(T)) is recognized as the golden standard to describe electronic structure, as long as no strong static correlation exists in the studied system. The drawback is that CCSD(T) is applicable only to small systems, since its cost scales as  $N^7$  with  $N$  being the basis set size of the system.

This has conveyed many efforts to reduce the computational cost of CCSD(T) by, for example, taking advantage of density fitting (or resolution of identity) approximations and new algorithms for two electron integrals transformation,<sup>29–32</sup> as well as using localized molecular orbitals<sup>33–36</sup> to optimize the selection of the most relevant excitations.<sup>37–40</sup> Thanks to these technical advancements, CCSD(T) is now affordable for systems up to 100 atoms, including transition metals. Although different implementations of linear scaling CCSD(T) are quite effective, we found the DLPNO–CCSD(T)<sup>34,35</sup> implementation the easiest to use for end users. DLPNO stands for domain-based local pair natural orbital, since instead of canonical delocalized orbitals, pair natural orbitals<sup>41</sup> are used and then localized,<sup>34,35</sup> so that they can be classified into domains for proper sorting and selection of the most important excitations accounting for electronic correlation.

Received: June 21, 2015

Published: August 27, 2015

DLPNO-CCSD(T) accuracy has been assessed on either full CCSD(T) or experimental data for some systems of interest including noncovalent interactions,<sup>32</sup> enzymatic reactions,<sup>42</sup> organic reactions<sup>42,43</sup> transition-metal-promoted reactions,<sup>44–47</sup> conformational issues in transition metal structures,<sup>44</sup> and even extended to solid oxide crystals<sup>48</sup> and a small protein.<sup>35</sup> However, in the majority of the cases the DLPNO-CCSD(T) method was validated against experimental data on transition metals reactions in solvent,<sup>44–47</sup> and consequently the accuracy of the combined DLPNO-CCSD(T) plus particular solvation model was assessed rather than the performance of DLPNO-CCSD(T) itself.

To test the performance of the DLPNO-CCSD(T) method from a different perspective, in the current work we present a systematic test study of the gas phase noncovalent ligand dissociation enthalpies in 72 complexes of  $\text{Cu}^+$ ,  $\text{Ag}^+$ , and  $\text{Au}^+$  related to catalysis. To assess the performance of the DLPNO-CCSD(T) method itself the following steps were taken. First, to eliminate the effect of the solvent, only gas phase measurements were used to build the test sets. Second, to discard the effects from the low-lying frequency modes, important for the molecular entropy, only performance in enthalpies was analyzed. Third, to exclude any influence of the vector relativistic effects, only complexes giving closed shell reactants and products were selected. Finally, to avoid systems with multireference character, T1 diagnostic values were thoroughly monitored.

## 2. COMPUTATIONAL DETAILS

The ORCA<sup>49</sup> suite of programs was employed for all the calculations performed in the present work.

**2.1. Geometry Optimizations.** The geometry optimization was performed using the pure GGA PBE<sup>50,51</sup> functional as implemented in ORCA. The Grimme's D3(BJ)<sup>52</sup> dispersion correction was activated via the "D3BJ" option to arrive at the PBE-D3(BJ) functional because some of the complexes from the benchmark set are not small (see Figure 1) and the inclusion of dispersion interactions during the optimization might be essential.<sup>53–55</sup> Default values were adopted for the self-consistent-field (SCF) and geometry optimization convergence criteria. Numerical integration of the exchange-correlation (XC) terms was performed using tighter-than-default "Grid 7" option (Lebedev770 and IntAcc = 5.67 and no FinalGrid) to eliminate potential numerical noise. Geometries were characterized as true energy minima by the eigenvalues of the analytically calculated Hessian matrix. Translational, rotational, and vibrational partition functions for thermal corrections to give total enthalpies were computed within the ideal-gas, rigid-rotor, and harmonic oscillator approximations following standard procedures.

The all-electron DEF2-TZVP<sup>56</sup> basis sets of the Karlsruhe group was used on all the elements apart from Ag and Au, along with corresponding auxiliary basis functions<sup>57</sup> needed to fit Coulomb potential to speed up the DFT calculations. Quasi-relativistic effective core potentials (ECP) of the Stuttgart type<sup>58</sup> were used to describe 28 inner electrons of Ag and 60 inner electrons of Au in combination with the corresponding DEF2-TZVP basis set.

Despite the complexes studied in the present work could be optimized with more rigorous WFT methods or more advanced hybrid meta-GGA DFT functionals, we found pure GGA DFT and density fitting algorithms more useful in light of its exclusive role in optimization of realistic-size TM complexes

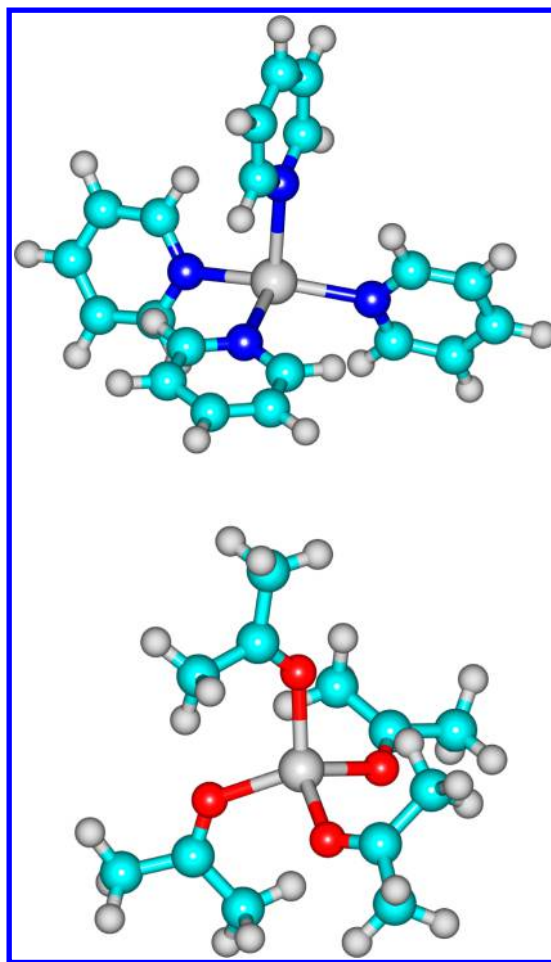


**Figure 1.** Molecular structures of the largest  $\text{Ag}^+$  (above) and  $\text{Cu}^+$  (below) complexes, which were investigated in the current work. Color coding: N (blue), C (turquoise), O (red), H (gray), Ag (gray), Cu (gray).

(>100 atoms). Indeed, the DLPNO-CCSD(T) method is aimed at molecules of this size, and its performance in conjunction with pure GGA for location of stationary points on the potential energy surface is especially interesting for routine applications.

If several conformations could be possible for some complexes, the structure of the most stable one was either taken from the literature or was found by geometry optimization with PBE functional of many manually generated conformations.

**2.2. Single-Point Energy Evaluations.** The DLPNO-CCSD(T)<sup>34,35</sup> method was applied for all single-point energy evaluations in the current work. The default "NormalPNO" DLPNO settings (TCutPairs =  $10^{-4}$ , TCutPNO =  $3.33 \times 10^{-7}$ , TCutMKN =  $10^{-3}$ ) were used as recommended for most computational applications in terms of cost/efficiency ratio.<sup>40</sup>

**2.2.1. Reactions Involving  $\text{Ag}^+$  and  $\text{Au}^+$  Complexes.** Fully relativistic ECP of the Stuttgart type<sup>59</sup> were used to describe 28 inner electrons of Ag and 60 inner electrons of Au in combination with the corresponding correlation consistent basis sets "CC-PVTZ-PP" and "CC-PVQZ-PP" of Peterson et al.<sup>60</sup> All other elements were described with all-electron correlation consistent basis sets of the CC-PVNZ<sup>61–63</sup> family ( $N = 3$  and 4). The correlation fitting basis sets (CC-PVNZ/C) developed by Hättig et al.<sup>64</sup> necessary for the resolution of

identity approximation (RI) as a part of DLPNO scheme were used. Non relativistic Hamiltonian was used for all the calculations involving silver and gold complexes. This combination of the basis sets will be further referred as “CC-PVNZ (ECP)”.

**2.2.2. Reactions Involving Cu<sup>+</sup> Complexes.** Depending on the degree of inclusion of the scalar relativistic effects few strategies have been employed to describe ligand dissociation in the copper complexes. All strategies involve correlation fitting basis sets (CC-PVNZ/C) developed by Hättig et al.<sup>64</sup> for RI approximation.

**2.2.2.1. All-Electron Nonrelativistic Calculations.** The nonrelativistic Hamiltonian was used in conjunction with all electron correlation consistent basis sets of CC-PVNZ (*N* = 3 and 4) family.<sup>61–63</sup> The copper atom was described with all electron basis set of Peterson et al.<sup>65</sup> This combination of the basis sets will be termed CC-PVNZ from thereafter.

**2.2.2.2. Effective Core Potential Calculations.** The non-relativistic Hamiltonian was used in conjunction with all electron correlation consistent basis sets of the CC-PVNZ (*N* = 3 and 4) family<sup>61–63</sup> on all the elements but copper. Fully relativistic ECPs of the Stuttgart type<sup>59</sup> were used to describe 10 inner electrons of Cu in combination with corresponding correlation consistent basis sets CC-PVTZ-PP and CC-PVQZ-PP of Peterson et al.<sup>60</sup> This combination of the ECP and the basis set corresponds to CC-PVNZ (ECP) strategy used earlier for silver complexes.

**2.2.2.3. Scalar Relativistic Calculations.** The scalar relativistic Douglas–Kroll–Hess (DKH)<sup>66</sup> Hamiltonian was applied as implemented in the ORCA suite of programs. All electron correlation consistent basis sets recontracted to be used in conjunction with DKH Hamiltonian were used.<sup>67</sup> This combination of the correlation consistent basis and DKH Hamiltonian will be termed CC-PVNZ (DKH).

**2.2.3. Complete Basis Set Extrapolation.** To eliminate the effects from basis set incompleteness, the extrapolation schemes for HF and correlation energies of individual species suggested by Helgaker et al.<sup>68–70</sup> for two adjacent CC-PVNZ level basis sets were employed:

$$E_{\text{HF}}^X = E_{\text{HF}}^\infty + \alpha e^{-1.63X} \quad (1)$$

$$E_{\text{corl}}^X = E_{\text{corl}}^\infty + \beta e^{-X} \quad (2)$$

where *X* = 3 and 4 for CC-PVTZ and CC-PVQZ basis sets, correspondingly; (*E*<sub>HF</sub><sup>∞</sup>/*E*<sub>corl</sub><sup>∞</sup>) HF and correlation energies at CBS limit; *α/β* are parameters to be obtained from a system of the two equations. The total bond dissociation enthalpy at CBS limit for each molecule AB was evaluated via equation

$$\begin{aligned} \Delta H_{\text{DLPNO-CCSD(T)}}^0 &= E_{\text{HF}}^\infty(A) + E_{\text{corl}}^\infty(A) + H_{\text{corr}}^{\text{PBE-D3}}(A) \\ &+ E_{\text{HF}}^\infty(B) + E_{\text{corl}}^\infty(B) + H_{\text{corr}}^{\text{PBE-D3}}(B) \\ &- (E_{\text{HF}}^\infty(AB) + E_{\text{corl}}^\infty(AB) + H_{\text{corr}}^{\text{PBE-D3}}(AB)) \end{aligned} \quad (3)$$

where *H*<sub>corr</sub><sup>PBE-D3</sup> is the correction to the electronic energy to arrive to the enthalpy, see section 2.1 for the details.

As for an indicative comparison with state of the art DFT functionals, we also evaluated M06 dissociation enthalpies on this study with equivalent basis sets. The formula we used for M06 CBS extrapolation being:

$$\begin{aligned} \Delta H_{\text{M06}}^0 &= E_{\text{M06}}^\infty(A) + H_{\text{corr}}^{\text{PBE-D3}}(A) + E_{\text{M06}}^\infty(B) \\ &+ H_{\text{corr}}^{\text{PBE-D3}}(B) - (E_{\text{M06}}^\infty(AB) + H_{\text{corr}}^{\text{PBE-D3}}(AB)) \end{aligned} \quad (4)$$

where *E*<sub>M06</sub><sup>∞</sup> has been extrapolated via formula 1.

As for the basis set superposition error (BSSE), the standard counterpoise correction (CP)<sup>71</sup> has not been applied in the present study for several reasons. First, with the two-point CBS extrapolation scheme<sup>68–70</sup> based on CC-PVTZ/CC-PVQZ basis sets we approach the limit of a complete basis set at which in theory both the BSSE and basis set incompleteness should be virtually reduced to zero. Indeed, the mean signed error obtained for all 72 dissociation reaction turned out to be close to practically zero kcal/mol (see below) while in case of strong pollution by BSSE large and positive MSE would take place. Moreover, considering the complete basis set as a reference, several studies show that the extrapolation scheme is either as<sup>72</sup> or more<sup>73</sup> accurate than the counterpoise correction for the evaluation of interaction energies and reaction barriers. Other references<sup>73–75</sup> also demonstrate a better accuracy of the extrapolation scheme over the counterpoise method for the evaluation of an experimental property. Finally, recent studies on CCSD(T) evaluation of metal–ligand bond dissociations do not include counterpoise corrections.<sup>46,76</sup>

**2.3. The Benchmark Set.** The DLPNO–CCSD(T) method in its current implementation can only be applied to closed shell systems. This puts an important constraint on the potential TM ion reactions to be included in the benchmark set: both reactants and products have to be singlets. Since a dominant part of the TM ions have unfilled d-shell, there is a high chance that open shell states of the complexes formed by these metals might be more stable comparing to closed shell states. To verify it manually for every TM complex is a daunting task, and even worse, the results can also be dependent on the method chosen. The 11 group metals such as Cu, Ag and Au are known to have one 4s electron on a top of the filled d-shell which leads to the closed shell d<sup>10</sup> configurations of the ions. Since the most stable closed-shell d<sup>10</sup> configuration is unlikely to be changed by closed-shell noncovalent ligands in the TM complexes, we decided to focus only on Cu<sup>+</sup>, Ag<sup>+</sup> and Au<sup>+</sup> complexes in the current work. In total for the current study we selected 33, 24, and 15 noncovalent gas phase binding enthalpies/ZPE-energies for Cu<sup>+</sup>, Ag<sup>+</sup>, and Au<sup>+</sup> complexes, respectively, for which reliable experimental data are available.

It should be noted that the dominant part of the experimental reaction energies are given as enthalpies at 298.15 K and other are zero-point corrected energies (ZPE). To keep the study consistent, all ZPE values were converted to enthalpies via following procedure. First, ZPE and enthalpic corrections were calculated at the PBE-D3(BJ)/DEF2-TZVP protocol, see above. Then, the subtraction of the ZPE correction from the experimental ZPE energies was followed by addition of the enthalpic correction to arrive at reaction enthalpies that were then compared to their experimental counterparts. If more than one experimental value was available for the reaction, the average was taken as the reference for comparisons with our calculations. To ensure that reactants and products are both singlets, the SP energy evaluations with multiplicities 3 (triplets) and 5 (quintet) at geometry optimization level were done on the optimized structures. In all cases the energies of open shell states were higher in energy. The selected dissociation reactions can be considered as a reference data set for further benchmarking in the future. The



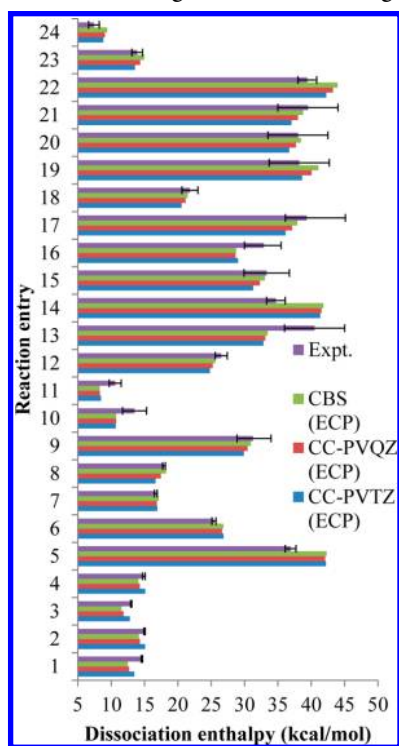
33, 24, and 15 noncovalent ligand dissociation reactions for  $\text{Cu}^+$ ,  $\text{Ag}^+$ , and  $\text{Au}^+$  thus compose data sets CUNCDE33, AGNCDE24, and AUNCDE15, all together combined to the G11NCDE72 data set. Optimized coordinates of all the systems composing these data sets are included in the [Supporting Information](#) and also available at the url: <https://sites.google.com/site/theochemdatasets>.

### 3. RESULTS AND DISCUSSION

First, we discuss the DLPNO-CCSD(T) performance on the ligand dissociation enthalpies of  $\text{Ag}^+$  complexes. Then, we proceed to the reactions involving  $\text{Cu}^+$  ions. A keen attention is paid to importance of scalar relativistic effects. After that, we discuss the results obtained for  $\text{Au}^+$  complexes. Finally, we comment on the overall performance obtained for all three coinage metal ion reactions both for DLPNO-CCSD(T) and M06 and practical information shall be given.

**3.1.  $\text{Ag}^+$  Bond Dissociation Enthalpies, the AGNCDE24 Data Set.** The DLPNO-CCSD(T) bond dissociation enthalpies obtained with CC-PVTZ (ECP), CC-PVQZ (ECP), and CBS (ECP) basis sets are presented in [Chart 1](#)

**Chart 1.** Experimental and DLPNO-CCSD(T)/CC-PVNZ (ECP) Dissociation Enthalpies Obtained for Transition Metal Ion–Noncovalent Ligand Bonds in 24  $\text{Ag}^+$  Complexes



along with the corresponding experimental values. In general, an accuracy in MUE below 3 kcal/mol has been achieved in reproducing the dissociation enthalpies for practically all the  $\text{Ag}^+$  complexes. Few dissociation enthalpies, however, are somewhat poorly reproduced; in particular large errors of 5.4, 7.0, 7.1, 4.1, and 4.5 kcal/mol were obtained for reactions 5, 13, 14, 16, and 22, respectively. To have a better understanding of an inconsistency between calculated numbers and their experimental counterparts, additional measurements of Deng and Kebarle<sup>103</sup> providing the total dissociation enthalpy of the two noncovalent ligands ( $\text{AgL}_2^+ = \text{Ag}^+ + \text{L}_2$ ) were analyzed.

In short, Deng and Kebarle estimated the sum of the enthalpies of reactions 13 and 17 (dissociation of the two benzene molecules from  $(\text{Ag} \cdot 2\text{C}_6\text{H}_6)^+$ ) to be  $68.2 \pm 3.0$  kcal/mol. The DLPNO-CCSD(T)/CBS (ECP) calculations predict this value to be 71.4 kcal/mol which is only slightly above the experimental values, and almost within the experimental uncertainty. Since the enthalpy of the reaction 17 is predicted quite well by our estimates, we believe that the dissociation enthalpy of the reaction 13 might be slightly overestimated in the experiments of Ho et al.<sup>81</sup> Also, our calculated reaction enthalpies 14 and 22 (acetonitrile dissociation from  $(\text{Ag} \cdot 2\text{C}_2\text{H}_3\text{N})^+$  and  $(\text{Ag} \cdot 2\text{C}_2\text{H}_3\text{N})^+$ ) are both overestimated comparing to the experimental measurements of Shoeib et al.<sup>82</sup> This results in overestimation of the sum of the enthalpies of reaction 14 and 22 by 11.6 kcal/mol relative to experimental value of Shoeib et al.<sup>82</sup> of 74.1. On the other hand, Deng and Kebarle<sup>103</sup> estimate the sum of the enthalpies of reaction 14 and 22 to be  $84.8 \pm 3.0$  kcal/mol, which is perfect agreement with our calculations.

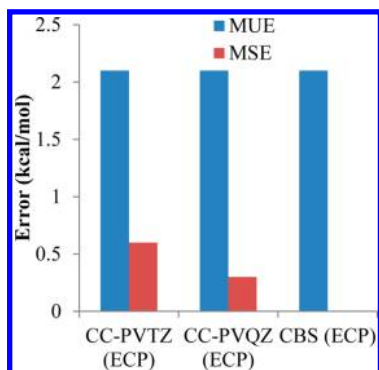
The enthalpy of reaction 16 (dissociation of  $\text{H}_2\text{O}$  molecule from  $(\text{Ag} \cdot \text{H}_2\text{O})^+$ ) is underestimated by our DLPNO-CCSD(T) calculations, and amounts to 28.7 kcal/mol at CBS (ECP) extrapolation while the experimental estimates are  $32.5 \pm 2.5$ <sup>83</sup> and  $33.3 \pm 2.2$  kcal/mol.<sup>77</sup> However, we predict the sum of the enthalpy of reactions 16 and 6 (dissociation of the two  $\text{H}_2\text{O}$  molecules from  $(\text{Ag} \cdot 2\text{H}_2\text{O})^+$ ) to be 55.6 kcal/mol, which matches perfectly the estimate of Deng and Kebarle<sup>103</sup> equal to  $56.5 \pm 3.0$  kcal/mol. Since the enthalpy of reaction 6 is predicted quite close to the measurements of Holland et al.<sup>77</sup> we believe that the enthalpy reported by Holland et al.<sup>77</sup> and Aribi et al.<sup>83</sup> for reaction 16 might be slightly overestimated.

The enthalpy of reaction 5 (dissociation of  $\text{NH}_3$  from  $(\text{Ag} \cdot 2\text{NH}_3)^+$ ) is calculated to be 42.3 kcal/mol, which is somewhat larger than 36.9 kcal/mol documented by Holland et al.<sup>77</sup> As for the binding of  $\text{NH}_3$  in  $(\text{Ag} \cdot \text{NH}_3)^+$ , our calculations predict corresponding dissociation enthalpy of 43.4 kcal/mol. Unfortunately, no experimental value is available on the dissociation of  $\text{NH}_3$  from  $(\text{Ag} \cdot \text{NH}_3)^+$  for a comparison. Nevertheless, our theoretical estimation of dissociation of the two  $\text{NH}_3$  molecules from  $(\text{Ag} \cdot 2\text{NH}_3)^+$  complex, 85.7 kcal/mol, is in perfect agreement with the experimental estimates of Deng and Kebarle ( $85.6 \pm 3.0$  kcal/mol).<sup>103</sup> Since pronounced overestimation of the enthalpy of reaction 5 has also been noticed in other DFT<sup>104</sup> and CCSD(T) calculations,<sup>105</sup> perhaps re-examination of the data of Holland et al. would be of interest.

Thus, we believe that in addition to the approximations used in the theoretical calculations, documented disagreements can also be attributed partly to the inconsistencies between different experimental measurements.

In [Chart 2](#) the overall errors obtained for the  $\text{Ag}^+$  data set are presented. With CC-PVTZ (ECP) basis set the MUE/MSE are equal to 2.1 and 0.6 kcal/mol, respectively. Upon the increase of the basis set to CC-PVQZ (ECP) quality the MUE remains the same and MSE gets equal to 0.3 demonstrating only a slight tendency to underestimation. Finally, at CBS limit the MUE gets equal 2.1 kcal/mol and MSE is 0.0 kcal/mol, indicating that the cases where enthalpies are overestimated are exactly compensated by the cases where the enthalpies are underestimated. Bearing in mind that average uncertainty associated with experimental enthalpies is in general near 1–2 kcal/mol we consider the achieved accuracy as acceptable. Another encouraging observation is that in terms of MUEs the results

Chart 2. DLPNO–CCSD(T)/CC-PVNZ (ECP) Mean Unsigned (MUE) and Mean Signed (MSE) Errors with Respect to Experimental Values Obtained for 24 Dissociation Enthalpies Involving Ag<sup>+</sup> Complexes



are converged already at CC-PVTZ (ECP) basis set making the calculations affordable for large TM complexes of hundreds of atoms.

### 3.2. Cu<sup>+</sup> Binding Enthalpies, the CUNCDE33 Data Set.

**3.2.1. Non Relativistic All Electron Calculations.** The DLPNO–CCSD(T) enthalpies calculated for dissociation of noncovalent ligands from Cu<sup>+</sup> complexes are given in Chart 3. Comparing to the performance obtained for Ag<sup>+</sup> complexes, a clear tendency to underestimation can be identified. This is especially pronounced if MUE and MSE are plotted for all 33 Cu<sup>+</sup> reactions, see Chart 4. Thus, with the CC-PVTZ basis set

Chart 3. Experimental and DLPNO–CCSD(T)/CC-PVNZ Dissociation Enthalpies Obtained for Transition Metal Ion–Noncovalent Ligand Bonds in 33 Cu<sup>+</sup> Complexes

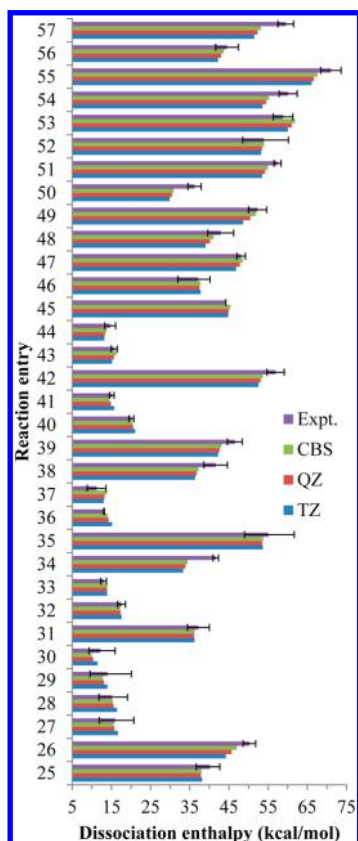
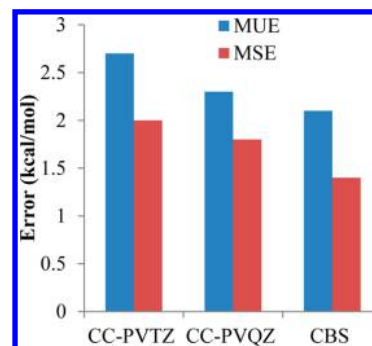


Chart 4. DLPNO–CCSD(T)/CC-PVNZ Mean Unsigned (MUE) and Mean Signed (MSE) Errors with Respect to Experimental Values Obtained for 33 Dissociation Enthalpies Involving Cu<sup>+</sup> Complexes



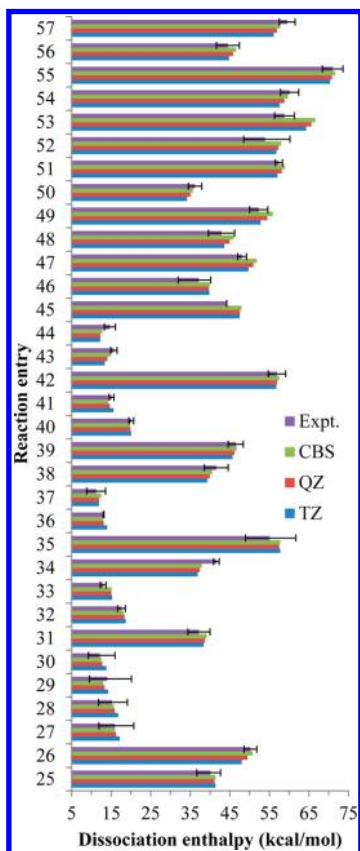
the MUE/MSE errors are equal to 2.7 and 2.0 kcal/mol which is considerably larger comparing to what was observed for Ag<sup>+</sup> complexes. Upon increase in the basis set to CC-PVQZ the MUE and MSE get improved only by 0.4 and 0.2 kcal/mol, respectively. Finally, at CBS extrapolation the MUE and MSE are equal to 2.1 and 1.4 kcal/mol, correspondingly. While MUE gets equal to what was obtained for Ag<sup>+</sup> complexes in the CBS limit, MSE does not vanish and remains equal to 1.4 kcal/mol, demonstrating that the dissociation enthalpies are systematically underestimated.

Since DLPNO–CCSD(T) estimates have been shown to be within 1 kcal/mol of CCSD(T) results,<sup>40</sup> truncation in the localization scheme is unlikely to be responsible for the underestimation as well as the basis sets which are of acceptable quality for the calculations at this level of theory. It is especially interesting that for seemingly trivial reaction 50 (CO dissociation from CuCO<sup>+</sup>) our documented enthalpy at the CBS limit is 30.9 kcal/mol, which is 5.3 kcal/mol than experimentally measured quantity. In principle, scalar relativistic effects, which are proportional to  $Z^{4.34}$  with  $Z$  being the atomic number, according to the Wood-Boring calculations<sup>106</sup> have been shown to be non-negligible for Cu, as documented in the literature.<sup>44,76,107–110</sup> Indeed, Matito et al.<sup>111</sup> estimated the CO bond dissociation energy in (CuCO)<sup>+</sup> to be equal 37.3 kcal/mol at CCSD(T) Dirac–Coulomb Hamiltonian level. On the other hand, Frenking et al.<sup>112</sup> using relativistic Stuttgart-type ECP on Cu atom estimated this energy to be 31.2 kcal/mol, which is more in line with our nonrelativistic estimates. However, for example, in the popular def2 family of the basis sets of Ahlrichs and co-workers<sup>56</sup> widely used for routine DFT and WFT calculations nowadays, relativistic ECPs start to be used only from Rb implying that the relativistic effects up to Kr could be neglected. Therefore, we believe that it is worth to explore the influence of scalar relativistic effects on Cu<sup>+</sup> bonding energies.

To further explore the influence of the scalar relativistic effects on the dissociation enthalpies of Cu<sup>+</sup> complexes we carried out DLPNO–CCSD(T) calculations with Stuttgart ECP on copper as well as all-electron relativistic calculations with the DKH Hamiltonian.

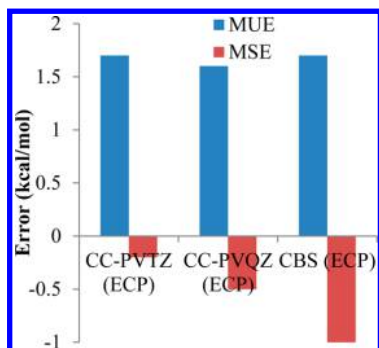
**3.2.2. Relativistic ECP Calculations.** The DLPNO–CCSD(T) results obtained with Stuttgart relativistic ECP on copper atom combined with the corresponding CC-PVNZ-PP basis set and Dunning CC-PVNZ basis sets on other elements are presented in Chart 5. The general tendency to underestimation of the dissociation enthalpies documented previously for Cu<sup>+</sup>

**Chart 5.** Experimental and DLPNO–CCSD(T)/CC-PVNZ (ECP) Dissociation Enthalpies Obtained for Transition Metal Ion–Noncovalent Ligand Bonds in 33  $\text{Cu}^+$  Complexes



complexes has disappeared. This is clear from inspection of Chart 6, in which the MUE and MSE are given for all 33  $\text{Cu}^+$  reactions. Already at CC-PVTZ (ECP) level the MUE and MSE errors are 1.7 kcal/mol and  $-0.2$  kcal/mol.

**Chart 6.** DLPNO–CCSD(T)/CC-PVNZ (ECP) Mean Unsigned (MUE) and Mean Signed (MSE) Errors with Respect to Experimental Values Obtained for 33 Dissociation Enthalpies Involving  $\text{Cu}^+$  Complexes



Comparing to all-electron “CC-PVTZ” results the MUE decreases by almost 1 kcal/mol while MSE is reduced by more than 1.5 kcal/mol, and is essentially vanishing. Upon the increase in the basis set to quadruple- $\zeta$  quality only minor ( $\sim 0.1$  kcal/mol) improvement in the MUE was achieved, while the MSE was increased to  $-0.5$  kcal/mol, underlying the

tendency to overestimate the enthalpies. Finally, at the CBS level the MUE is 1.7 kcal/mol and the MSE is  $-1.0$  kcal/mol.

It should also be mentioned that for all-electron CBS dissociation enthalpies MUEs larger than 4.0 kcal/mol were found for 5 reactions (34, 38, 50, 54, 57), whereas using ECP on copper results in a MUE larger than 4 kcal/mol only for reaction 53. For this reaction the DLPNO–CCSD(T)/CBS(ECP) calculations predict the enthalpy change to be 7.8 kcal/mol larger than the experimental estimates of Rodgers et al.<sup>96</sup> However, we believe that such large disagreement cannot be ascribed only to the approximations associated with our calculations. Indeed, alternative photodissociation threshold measurements<sup>113</sup> predict enthalpy of reaction 53 to be  $\sim 65.1$  kcal/mol (enthalpy corrected) which is only 1.5 kcal/mol lower than our theoretical estimate. Usually, photodissociation measured enthalpies are less reliable than measured collision induced dissociation enthalpies, and that is why only latter are included in Table 1 to calibrate the DLPNO–CCSD(T) performance. Probably, the experimental collision induced dissociation enthalpy value for reaction 53 should be re-examined.

Importantly, the problematic reaction 50 for which larger errors were documented with all-electron nonrelativistic basis sets is now perfectly described with the MUE/MSE in CBS limit equal to 0.5 kcal/mol. The dissociation enthalpy of reaction 50 is 35.7 kcal/mol, which essentially matches the experimental value of  $36.2 \pm 1.7$  kcal/mol by Meyer and co-authors.<sup>80</sup> While this result is in close agreement with the relativistic calculations of Matito et al.,<sup>111</sup> it differs from the estimate of Frenking et al.<sup>112</sup> by 4.5 kcal/mol. This difference can be explained by better correlation consistent basis sets and CBS extrapolation used in the present work. It should also be mentioned that the difference between relativistic (ECP) and nonrelativistic all electron enthalpies is especially impressive for reaction 50 since it amounts to 4.8 kcal/mol.

**3.2.3. Relativistic All Electron Douglass–Kroll–Hess Calculations.** To ensure that the difference between ECP and all-electron results are due to relativistic effects, we performed DLPNO–CCSD(T) DKH calculations with “CC-PVTZ-DKH” basis sets which were recontracted<sup>67</sup> to be used for the DKH calculations. It must be noted that both the number and the values of the exponents are identical in the CC-PVNZ-DKH to those in the CC-PVNZ basis sets. The only difference between CC-PVNZ and CC-PVNZ-DKH basis sets is the contraction coefficients, which means that the basis sets of CC-PVNZ and CC-PVNZ-DKH are exactly of the same quality.

The absolute reaction enthalpies with DKH calculations turned out to be very similar to those obtained using ECP on copper and are given in Charts S1 and S2 (see Supporting Information). The MUE/MSEs obtained for all 33  $\text{Cu}^+$  reactions are similar to the MUE/MSE obtained with ECP. The average unsigned difference between dissociation energies obtained with ECP and all-electron DKH results are 0.2, 0.1, and 0.2 kcal/mol for CC-PVTZ, CC-PVQZ, and CBS basis sets. This confirms that the difference documented between ECP and all-electron nonrelativistic results is almost entirely due to relativistic effects. Moreover, the relativistic contribution to the reaction energies is not uniform for all the reactions. The difference between ( $\Delta E(\text{DLPNO–CCSD(T)}/\text{CBS}(\text{DKH}))$  and  $\Delta E(\text{DLPNO–CCSD(T)}/\text{CBS})$ ) strongly depends on the reactions, it varies from  $-1.7$  kcal/mol (reaction 43) to 5.1 kcal/mol (reaction 57). This underlines that the relativistic



Table 1. Experimental Dissociation Enthalpies/Energies Used for Benchmarking of DLPNO–CCSD(T) Calculations

no.	reaction	expt. $\Delta H^\circ$ (298.15) or $D_0$ (kcal/mol) <sup>a</sup>	av $\Delta H^\circ$ (298.15) (kcal/mol) <sup>b,c</sup>
1	$(\text{Ag}\cdot 3\text{H}_3\text{N})^+ = (\text{Ag}\cdot 2\text{H}_3\text{N})^+ + \text{H}_3\text{N}$	$14.6 \pm 0.1^{77}$	$14.6 \pm 0.1$
2	$(\text{Ag}\cdot 3\text{H}_2\text{O})^+ = (\text{Ag}\cdot 2\text{H}_2\text{O})^+ + \text{H}_2\text{O}$	$15.0 \pm 0.1^{77}$	$15.0 \pm 0.1$
3	$(\text{Ag}\cdot 4\text{H}_3\text{N})^+ = (\text{Ag}\cdot 3\text{H}_3\text{N})^+ + \text{H}_3\text{N}$	$13.0 \pm 0.1^{77}$	$13.0 \pm 0.1$
4	$(\text{Ag}\cdot 4\text{H}_2\text{O})^+ = (\text{Ag}\cdot 3\text{H}_2\text{O})^+ + \text{H}_2\text{O}$	$14.9 \pm 0.2^{77}$	$14.9 \pm 0.2$
5	$(\text{Ag}\cdot 2\text{H}_3\text{N})^+ = (\text{Ag}\cdot \text{H}_3\text{N})^+ + \text{H}_3\text{N}$	$36.9 \pm 0.8^{77}$	$36.9 \pm 0.8$
6	$(\text{Ag}\cdot 2\text{H}_2\text{O})^+ = (\text{Ag}\cdot \text{H}_2\text{O})^+ + \text{H}_2\text{O}$	$25.4 \pm 0.3^{77}$	$25.4 \pm 0.3$
7	$(\text{Ag}\cdot 3\text{C}_5\text{H}_5\text{N})^+ = (\text{Ag}\cdot 2\text{C}_5\text{H}_5\text{N})^+ + \text{C}_5\text{H}_5\text{N}$	$16.7 \pm 0.2^{77}$	$16.7 \pm 0.2$
8	$(\text{Ag}\cdot 4\text{C}_5\text{H}_5\text{N})^+ = (\text{Ag}\cdot 3\text{C}_5\text{H}_5\text{N})^+ + \text{C}_5\text{H}_5\text{N}$	$17.9 \pm 0.2^{77}$	$17.9 \pm 0.2$
9	$(\text{Ag}\cdot 2\text{C}_2\text{H}_4)^+ = (\text{Ag}\cdot \text{C}_2\text{H}_4)^+ + \text{C}_2\text{H}_4$	$32.4 \pm 1.5;^{78} 30.1 \pm 1.3 (30.1 \pm 1.3 \text{ (ZPE)})^{79}$	$31.3(+2.7/-2.4)$
10	$(\text{Ag}\cdot 3\text{CO})^+ = (\text{Ag}\cdot 2\text{CO})^+ + \text{CO}$	$13.5 \pm 1.8 (13.1 \pm 1.8 \text{ (ZPE)})^{80}$	$13.5 \pm 1.8$
11	$(\text{Ag}\cdot 4\text{CO})^+ = (\text{Ag}\cdot 3\text{CO})^+ + \text{CO}$	$10.6 \pm 0.9 (10.8 \pm 0.9 \text{ (ZPE)})^{80}$	$10.6 \pm 0.9$
12	$(\text{Ag}\cdot 2\text{CO})^+ = (\text{Ag}\cdot \text{CO})^+ + \text{CO}$	$26.5 \pm 0.9 (26.1 \pm 0.9 \text{ (ZPE)})^{80}$	$26.5 \pm 0.9$
13	$(\text{Ag}^+ \cdot 2\text{C}_6\text{H}_6)^+ = (\text{Ag}\cdot \text{C}_6\text{H}_6)^+ + \text{C}_6\text{H}_6$	$40.5 \pm 4.5(39.9 \pm 4.5 \text{ (ZPE)})^{81}$	$40.5 \pm 4.5$
14	$(\text{Ag}\cdot 2\text{C}_2\text{H}_3\text{N})^+ = (\text{Ag}\cdot \text{C}_2\text{H}_3\text{N})^+ + \text{C}_2\text{H}_3\text{N}$	$34.7 \pm 1.4^{82}$	$34.7 \pm 1.4$
15	$(\text{Ag}\cdot \text{C}_2\text{H}_4)^+ = \text{Ag}^+ + \text{C}_2\text{H}_4$	$33.7 \pm 3;^{78} 32.9 \pm 3.0 (32.2 \pm 3 \text{ (ZPE)})^{79}$	$33.3(+3.4/-3.7)$
16	$(\text{Ag}\cdot \text{H}_2\text{O})^+ = \text{Ag}^+ + \text{H}_2\text{O}$	$32.5 \pm 2.5 (31.6 \pm 2.5 \text{ (ZPE)});^{83} 33.3 \pm 2.2^{77}$	$32.9(+2.6/-2.9)$
17	$(\text{Ag}\cdot \text{C}_6\text{H}_6)^+ = \text{Ag}^+ + \text{C}_6\text{H}_6$	$38.0 \pm 1.7 (37.3 \pm 1.7 \text{ (ZPE)});^{84} 40.6 \pm 4.5 (39.9 \pm 4.5 \text{ (ZPE)})^{81}$	$39.3(+6.0/-3.2)$
18	$(\text{Ag}\cdot \text{CO})^+ = \text{Ag}^+ + \text{CO}$	$21.8 \pm 1.2 (21.2 \pm 1.2 \text{ (ZPE)})^{80}$	$21.8 \pm 1.2$
19	$(\text{Ag}\cdot \text{C}_5\text{H}_{10})^+ = \text{Ag}^+ + \text{C}_5\text{H}_{10}$	$38.2 \pm 4.5 (37.8 \pm 4.5 \text{ (ZPE)})^{81}$	$38.2 \pm 4.5$
20	$(\text{Ag}\cdot \text{C}_3\text{H}_6\text{O})^+ = \text{Ag}^+ + \text{C}_3\text{H}_6\text{O}$	$38.0 \pm 4.5 (38.2 \pm 4.5 \text{ (ZPE)})^{81}$	$38.0 \pm 4.5$
21	$(\text{Ag}\cdot \text{C}_5\text{H}_8)^+ = \text{Ag}^+ + \text{C}_5\text{H}_8$	$39.5 \pm 4.5 (39.2 \pm 4.5 \text{ (ZPE)})^{81}$	$39.5 \pm 4.5$
22	$(\text{Ag}\cdot \text{C}_2\text{H}_3\text{N})^+ = \text{Ag}^+ + \text{C}_2\text{H}_3\text{N}$	$39.4 \pm 1.4^{82}$	$39.4 \pm 1.4$
23	$(\text{Ag}\cdot 3(\text{C}_2\text{H}_4))^+ = (\text{Ag}\cdot 2(\text{C}_2\text{H}_4))^+ + \text{C}_2\text{H}_4$	$13.9 \pm 0.8 (13.6 \pm 0.8 \text{ (ZPE)})^{79}$	$13.9 \pm 0.8$
24	$(\text{Ag}\cdot 4(\text{C}_2\text{H}_4))^+ = (\text{Ag}\cdot 3(\text{C}_2\text{H}_4))^+ + \text{C}_2\text{H}_4$	$7.4 \pm 0.8 (6.5 \pm 0.8 \text{ (ZPE)})^{79}$	$7.4 \pm 0.8$
25	$(\text{Cu}\cdot 2\text{H}_2\text{O})^+ = (\text{Cu}\cdot \text{H}_2\text{O})^+ + \text{H}_2\text{O}$	$39.6 \pm 3.0 (39 \pm 3.0 \text{ (ZPE)});^{85} 40.7 \pm 1.6^{86}$	$40.1(+2.5/-3.5)$
26	$(\text{Cu}\cdot 2\text{C}_3\text{H}_6\text{O})^+ = (\text{Cu}\cdot \text{C}_3\text{H}_6\text{O})^+ + \text{C}_3\text{H}_6\text{O}$	$50.2 \pm 1.6^{87}$	$50.2 \pm 1.6$
27	$(\text{Cu}\cdot 3\text{H}_2\text{O})^+ = (\text{Cu}\cdot 2\text{H}_2\text{O})^+ + \text{H}_2\text{O}$	$17.7 \pm 3.0 (17.0 \pm 3.0 \text{ (ZPE)});^{85} 13.7 \pm 1.8;^{86} 16.4 \pm 0.2^{77}$	$15.9(+4.8/-4.0)$
28	$(\text{Cu}\cdot 4\text{H}_2\text{O})^+ = (\text{Cu}\cdot 3\text{H}_2\text{O})^+ + \text{H}_2\text{O}$	$16.1 \pm 3.0 (15.0 \pm 3.0 \text{ (ZPE)});^{85} 12.8 \pm 1.0;^{86} 16.7 \pm 0.2^{77}$	$15.2(+3.9/-3.4)$
29	$(\text{Cu}\cdot 3\text{H}_3\text{N})^+ = (\text{Cu}\cdot 2\text{H}_3\text{N})^+ + \text{H}_3\text{N}$	$11.0 \pm 1.5;^{88} 17.0 \pm 3.1;^{89} 14.1 \pm 0.2^{77}$	$14.0(+6.1/-4.5)$
30	$(\text{Cu}\cdot 4\text{H}_3\text{N})^+ = (\text{Cu}\cdot 3\text{H}_3\text{N})^+ + \text{H}_3\text{N}$	$10.8 \pm 1.5;^{88} 12.9 \pm 3.1;^{89} 12.8 \pm 0.2^{77}$	$12.2(+3.8/-2.9)$
31	$(\text{Cu}\cdot 2\text{C}_6\text{H}_6)^+ = (\text{Cu}\cdot \text{C}_6\text{H}_6)^+ + \text{C}_6\text{H}_6$	$37.2 \pm 2.8 (37.1 \pm 2.8 \text{ (ZPE)})^{90}$	$37.2 \pm 2.8$
32	$(\text{Cu}\cdot 3\text{CO})^+ = (\text{Cu}\cdot 2\text{CO})^+ + \text{CO}$	$17.6 \pm 1.0 (18.0 \pm 1.0 \text{ (ZPE)})^{80}$	$17.6 \pm 1.0$
33	$(\text{Cu}\cdot 4\text{CO})^+ = (\text{Cu}\cdot 3\text{CO})^+ + \text{CO}$	$13.0 \pm 0.7 (12.7 \pm 0.7 \text{ (ZPE)})^{80}$	$13.0 \pm 0.7$
34	$(\text{Cu}\cdot 2\text{CO})^+ = (\text{Cu}\cdot \text{CO})^+ + \text{CO}$	$41.6 \pm 0.7 (41.0 \pm 0.7 \text{ (ZPE)})^{80}$	$41.6 \pm 0.7$
35	$(\text{Cu}\cdot 2\text{H}_3\text{N})^+ = (\text{Cu}\cdot \text{H}_3\text{N})^+ + \text{H}_3\text{N}$	$59.3 \pm 2.4;^{88} 52.1 \pm 3.1;^{91} 53.8 \pm 3.1^{77}$	$55.1(+6.6/-6.1)$
36	$(\text{Cu}\cdot 3\text{C}_2\text{H}_6\text{O})^+ = (\text{Cu}\cdot 2\text{C}_2\text{H}_6\text{O})^+ + \text{C}_2\text{H}_6\text{O}$	$13.1 \pm 1.0 (13.1 \pm 1.0 \text{ (ZPE)})^{92}$	$13.1 \pm 0.1$
37	$(\text{Cu}\cdot 4\text{C}_2\text{H}_6\text{O})^+ = (\text{Cu}\cdot 3\text{C}_2\text{H}_6\text{O})^+ + \text{C}_2\text{H}_6\text{O}$	$11.2 \pm 2.4 (10.8 \pm 2.4 \text{ (ZPE)})^{92}$	$11.2 \pm 2.4$
38	$(\text{Cu}\cdot 2\text{C}_2\text{H}_4)^+ = (\text{Cu}\cdot \text{C}_2\text{H}_4)^+ + \text{C}_2\text{H}_4$	$41.6 \pm 3.0 (41.5 \pm 3.0 \text{ (ZPE)})^{93}$	$41.6 \pm 3.0$
39	$(\text{Cu}\cdot 2\text{C}_2\text{H}_6\text{O})^+ = (\text{Cu}\cdot \text{C}_2\text{H}_6\text{O})^+ + \text{C}_2\text{H}_6\text{O}$	$46.5 \pm 1.9 (46.1 \pm 1.9 \text{ (ZPE)})^{92}$	$46.5 \pm 1.9$
40	$(\text{Cu}\cdot 3\text{C}_2\text{H}_3\text{N})^+ = (\text{Cu}\cdot 2\text{C}_2\text{H}_3\text{N})^+ + \text{C}_2\text{H}_3\text{N}$	$20.1 \pm 0.6^{94}$	$20.1 \pm 0.6$
41	$(\text{Cu}\cdot 4\text{C}_2\text{H}_3\text{N})^+ = (\text{Cu}\cdot 3\text{C}_2\text{H}_3\text{N})^+ + \text{C}_2\text{H}_3\text{N}$	$15.1 \pm 0.6^{94}$	$15.1 \pm 0.6$
42	$(\text{Cu}\cdot 2\text{C}_2\text{H}_3\text{N})^+ = (\text{Cu}\cdot \text{C}_2\text{H}_3\text{N})^+ + \text{C}_2\text{H}_3\text{N}$	$56.9 \pm 2.2^{94}$	$56.9 \pm 2.2$
43	$(\text{Cu}\cdot 3\text{C}_3\text{H}_6\text{O})^+ = (\text{Cu}\cdot 2\text{C}_3\text{H}_6\text{O})^+ + \text{C}_3\text{H}_6\text{O}$	$15.7 \pm 0.8^{94}$	$15.7 \pm 0.8$
44	$(\text{Cu}\cdot 4\text{C}_3\text{H}_6\text{O})^+ = (\text{Cu}\cdot 3\text{C}_3\text{H}_6\text{O})^+ + \text{C}_3\text{H}_6\text{O}$	$14.7 \pm 1.4^{94}$	$14.7 \pm 1.4$
45	$(\text{Cu}\cdot 2\text{C}_4\text{H}_5\text{N})^+ = (\text{Cu}\cdot \text{C}_4\text{H}_5\text{N})^+ + \text{C}_4\text{H}_5\text{N}$	$44.2 (44.0 \text{ (ZPE)})^{95}$	$44.2$
46	$(\text{Cu}\cdot \text{H}_2\text{O})^+ = \text{Cu}^+ + \text{H}_2\text{O}$	$35.9 \pm 3.0 (35 \pm 3.0 \text{ (ZPE)});^{85} 38.4 \pm 1.8^{86}$	$37.2 (+3.0/-5.2)$
47	$(\text{Cu}\cdot \text{C}_3\text{H}_6\text{O})^+ = \text{Cu}^+ + \text{C}_3\text{H}_6\text{O}$	$48.1 \pm 1.1^{87}$	$48.1 \pm 1.1$
48	$(\text{Cu}\cdot \text{C}_2\text{H}_4)^+ = \text{Cu}^+ + \text{C}_2\text{H}_4$	$42.9 \pm 3.3 (42.0 \pm 3.3 \text{ (ZPE)})^{93}$	$42.9 \pm 3.3$
49	$(\text{Cu}\cdot \text{C}_6\text{H}_6)^+ = \text{Cu}^+ + \text{C}_6\text{H}_6$	$52.3 \pm 2.3 (52.1 \pm 2.3 \text{ (ZPE)})^{90}$	$52.3 \pm 2.3$
50	$(\text{Cu}\cdot \text{CO})^+ = \text{Cu}^+ + \text{CO}$	$36.2 \pm 1.7 (35.5 \pm 1.7 \text{ (ZPE)})^{80}$	$36.2 \pm 1.7$
51	$(\text{Cu}\cdot \text{C}_2\text{H}_3\text{N})^+ = \text{Cu}^+ + \text{C}_2\text{H}_3\text{N}$	$57.4 \pm 0.9^{94}$	$57.4 \pm 0.9$
52	$(\text{Cu}\cdot \text{H}_3\text{N})^+ = \text{Cu}^+ + \text{H}_3\text{N}$	$56.6 \pm 3.6;^{88} 51.6 \pm 3.1;^{89} 53.5 \pm 3.1^{77}$	$53.9(+6.3/-5.4)$
53	$(\text{Cu}\cdot \text{C}_5\text{H}_5\text{N})^+ = \text{Cu}^+ + \text{C}_5\text{H}_5\text{N}$	$58.8 \pm 2.5^{96}$	$58.8 \pm 2.5$
54	$(\text{Cu}\cdot \text{C}_4\text{H}_4\text{N}_2)^+ = \text{Cu}^+ + \text{C}_4\text{H}_4\text{N}_2$	$60.1 \pm 2.3^{97}$	$60.1 \pm 2.3$
55	$(\text{Cu}\cdot \text{C}_5\text{H}_5\text{N}_5)^+ = \text{Cu}^+ + \text{C}_5\text{H}_5\text{N}_5$	$71.0 \pm 2.6 (70.3 \pm 2.6 \text{ (ZPE)})^{98}$	$71.0 \pm 2.6$
56	$(\text{Cu}\cdot \text{C}_2\text{H}_6\text{O})^+ = \text{Cu}^+ + \text{C}_2\text{H}_6\text{O}$	$44.5 \pm 2.9 (44.2 \pm 2.9 \text{ (ZPE)})^{92}$	$44.5 \pm 2.9$
57	$(\text{Cu}\cdot \text{C}_4\text{H}_5\text{N})^+ = \text{Cu}^+ + \text{C}_4\text{H}_5\text{N}$	$59.5 \pm 2.0 (59.0 \pm 2.0 \text{ (ZPE)})^{95}$	$59.5 \pm 2.0$
58	$(\text{Au}\cdot \text{styrene})^+ = \text{Au}^+ + \text{styrene}$	$44.0 \pm 0.9 (42.7 \pm 0.9 \text{ (ZPE)})^{99}$	$44.0 \pm 0.9$
59	$(\text{Au}\cdot \text{phenylacetylene})^+ = \text{Au}^+ + \text{phenylacetylene}$	$44.3 \pm 0.9 (43.1 \pm 0.9 \text{ (ZPE)})^{99}$	$44.3 \pm 0.9$
60	$(\text{Au}\cdot \text{C}_6\text{H}_6)^+ = \text{Au}^+ + \text{C}_6\text{H}_6$	$39.3 \pm 0.7 (38.7 \pm 0.7 \text{ (ZPE)})^{99}$	$39.3 \pm 0.7$

Table 1. continued

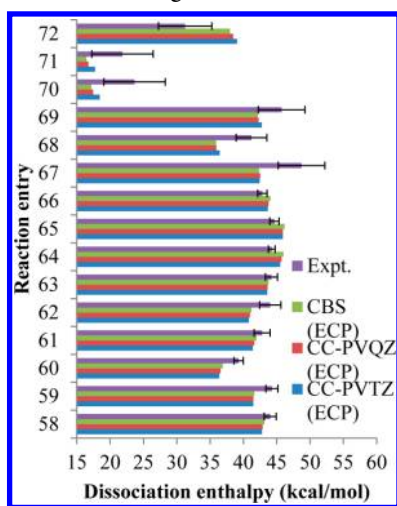
no.	reaction	expt. $\Delta H^\circ$ (298.15) or $D_0$ (kcal/mol) <sup>a</sup>	av $\Delta H^\circ$ (298.15) (kcal/mol) <sup>b,c</sup>
61	(Au-1-pentene) <sup>+</sup> = Au <sup>+</sup> + 1-pentene	42.8 ± 1.2 (42.0 ± 1.2 (ZPE)) <sup>99</sup>	42.8 ± 1.2
62	(Au-1-pentyne) <sup>+</sup> = Au <sup>+</sup> + 1-pentyne	44.0 ± 1.6 (43.4 ± 1.6 (ZPE)) <sup>99</sup>	44.0 ± 1.6
63	(Au-2-pentyne) <sup>+</sup> = Au <sup>+</sup> + 2-pentyne	44.2 ± 0.9 (44.0 ± 0.9 (ZPE)) <sup>99</sup>	44.2 ± 0.9
64	(Au-cyclooctane) <sup>+</sup> = Au <sup>+</sup> + cyclooctane	44.2 ± 0.5 (43.6 ± 0.5 (ZPE)) <sup>99</sup>	44.2 ± 0.5
65	(Au-1,5-cyclooctadiene) <sup>+</sup> = Au <sup>+</sup> + 1,5-cyclooctadiene	44.6 ± 0.7 (44.5 ± 0.7 (ZPE)) <sup>99</sup>	44.6 ± 0.7
66	(Au-1,3-cyclooctadiene) <sup>+</sup> = Au <sup>+</sup> + 1,5-cyclooctadiene	42.8 ± 0.7 (42.2 ± 0.7 (ZPE)) <sup>99</sup>	42.8 ± 0.7
67	(Au-CO) <sup>+</sup> = Au <sup>+</sup> + CO	48.7 ± 3.5 (48.0 ± 3.5 (ZPE)) <sup>100</sup>	48.7 ± 3.5
68	(Au-H <sub>2</sub> O) <sup>+</sup> = Au <sup>+</sup> + H <sub>2</sub> O	41.2 ± 2.3 (40.1 ± 2.3 (ZPE)) <sup>101</sup>	41.2 ± 2.3
69	(Au-2H <sub>2</sub> O) <sup>+</sup> = (Au-H <sub>2</sub> O) <sup>+</sup> + H <sub>2</sub> O	45.7 ± 3.5 (45.0 ± 3.5 (ZPE)) <sup>101</sup>	45.7 ± 3.5
70	(Au-3H <sub>2</sub> O) <sup>+</sup> = (Au-2H <sub>2</sub> O) <sup>+</sup> + H <sub>2</sub> O	23.7 ± 4.6 (23.1 ± 4.6 (ZPE)) <sup>101</sup>	23.7 ± 4.6
71	(Au-4H <sub>2</sub> O) <sup>+</sup> = (Au-3H <sub>2</sub> O) <sup>+</sup> + H <sub>2</sub> O	21.8 ± 4.6 (20.8 ± 4.6 (ZPE)) <sup>101</sup>	21.8 ± 4.6
72	(Au-C <sub>6</sub> F <sub>5</sub> H) <sup>+</sup> = Au <sup>+</sup> + C <sub>6</sub> F <sub>5</sub> H	31.2 ± 4.0 (31.0 ± 4.0 (ZPE)) <sup>102</sup>	31.2 ± 4.0

<sup>a</sup>Denoted as (ZPE). <sup>b</sup>Final average of experimental enthalpies  $\Delta H^\circ$ (298.15) used to compare with theoretical values. <sup>c</sup>To account for uncertainties if more than one experimental value is available, we considered the reference higher uncertainty as the difference between (1) the highest experimental enthalpy plus its corresponding positive uncertainty and (2) the average of the experimental values. As well, we considered the reference lower uncertainty as the difference between (1) the lowest experimental uncertainty plus its corresponding negative uncertainty and (2) the average of the experimental values.

effects cannot be ignored at least for Cu complexes if highly accurate absolute or relative dissociation reaction energies are of importance.

**3.3. Au<sup>+</sup> Bond Dissociation Enthalpies, the AUNCDE15 Data Set.** The DLPNO-CCSD(T) bond dissociation enthalpies obtained with CC-PVTZ (ECP), CC-PVQZ (ECP), and CBS (ECP) basis sets for 15 Au<sup>+</sup> complexes are presented in Chart 7 along with the corresponding

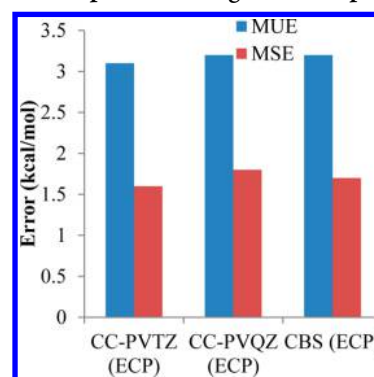
Chart 7. Experimental and DLPNO-CCSD(T)/CC-PVNZ (ECP) Dissociation Enthalpies Obtained for Transition Metal Ion–Noncovalent Ligand Bonds in 15 Au<sup>+</sup> Complexes



experimental values. Comparing to the results obtained for Ag<sup>+</sup> and Cu<sup>+</sup> complexes larger discrepancies between our theoretical estimates and the experimental dissociation enthalpies can be noticed. Indeed, the overall MUE and MSE errors in CBS limit obtained for all 15 enthalpies are 3.2 and 1.7 kcal/mol, respectively, as shown in Chart 8.

However, the error between our theoretical estimates and the experimental values is not equally spread for 15 reactions. The smallest errors have been obtained for reactions 58–66. Thus, MUE/MSE calculated only for those reactions are 1.6 and 0.6 kcal/mol, which is comparable to what was obtained for Cu<sup>+</sup> and Ag<sup>+</sup> complexes. Interestingly, the experimental uncertain-

Chart 8. DLPNO-CCSD(T)/CC-PVNZ (ECP) Mean Unsigned (MUE) and Mean Signed (MSE) Errors with Respect to Experimental Values Obtained for 15 Dissociation Enthalpies Involving Au<sup>+</sup> Complexes



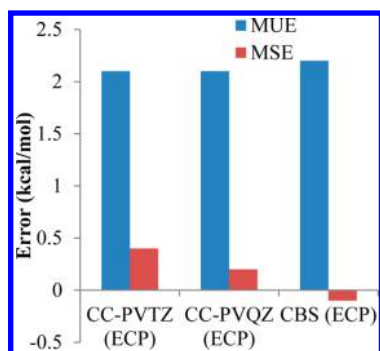
ties for the reactions 58–66 are in the range of 0.5–1.6 kcal/mol (average expt. uncertainty for these 9 reactions is 0.9 kcal/mol). On the other hand, for the reactions 67–72 significantly larger experimental uncertainties are documented, namely 2.3–4.6 kcal/mol (average expt. uncertainty for these 6 reactions is 3.8 kcal/mol). This indicates that larger errors obtained for reactions 67–72 are not necessarily related to theoretical method itself but can be consequence of larger experimental uncertainties and less precise measurements. Comparison of our study with other theoretical studies supports this hypothesis. For reaction 67 (dissociation of CO from AuCO<sup>+</sup>), our CBS estimate is 42.3 kcal/mol, which is 6.4 kcal/mol smaller comparing to measurements of Schwarz et al.<sup>100</sup> of 48.7 ± 3.5. Gordon and co-workers<sup>114</sup> have estimated the CO dissociation energy from AuCO<sup>+</sup> to be  $\Delta E_0 = 43.9$  kcal/mol at essentially CCSD(T)/aug-CC-PVTZ level (ECP on Au) which results in a final enthalpy  $\Delta H^\circ = 44.7$  kcal/mol after our enthalpic correction is applied. Schwarz et al.<sup>115</sup> estimated CO binding energy in AuCO<sup>+</sup> to be 44.1 kcal/mol ( $\Delta H^\circ = 44.9$  kcal/mol) at similar level of theory. Since both literature-based AuCO<sup>+</sup> dissociation enthalpies are neither CP-corrected, nor CBS-extrapolated, it is reasonable to assume that due to BSSE these values should be reduced by 1–2 kcal/mol, which would result in perfect agreement with our estimation. In



addition, for reaction 67 we also tested the influence of diffuse functions. Thus, our DLPNO-CCSD(T) aug-CC-PVTZ/aug-CC-PVQZ extrapolation results in the dissociation enthalpy of 42.5 kcal/mol which indicates that the diffuse functions, as expected for cationic systems, are not responsible for our deviations with the experimental measurements. Our CBS estimates for reactions 68, 69, 70, and 71 (dissociation of  $\text{H}_2\text{O}$  from  $\text{Au}(\text{H}_2\text{O})^+$ ,  $\text{Au}(\text{H}_2\text{O})_2^+$ ,  $\text{Au}(\text{H}_2\text{O})_3^+$ ,  $\text{Au}(\text{H}_2\text{O})_4^+$ ) are 35.9, 42.1, 17.2, and 16.5 kcal/mol, respectively. The experimental dissociation enthalpies of reactions 68–71 are systematically higher, namely, 41.2, 45.7, 23.7, and 21.8 kcal/mol. On the other hand, our DLPNO-CCSD(T) evaluations agree reasonably well with CCSD(T)/aVDZ estimates of Lee et al.:<sup>116</sup> 36.2, 41.7, 17.3, and 16.0 kcal/mol.

**3.4. Overall Performance.** 3.4.1. *DLPNO-CCSD(T).* The overall performance of the DLPNO-CCSD(T) method obtained for 72 transition metal ion ( $\text{Cu}^+$ ,  $\text{Ag}^+$ , and  $\text{Au}^+$ )–noncovalent ligands enthalpies is depicted in Chart 9. For

**Chart 9.** DLPNO-CCSD(T)/CC-PVNZ (ECP) Mean Unsigned (MUE) and Mean Signed (MSE) Errors with Respect to Experimental Values Obtained for All 72 Dissociation Enthalpies Involving  $\text{Cu}^+$ ,  $\text{Ag}^+$ , and  $\text{Au}^+$  Complexes

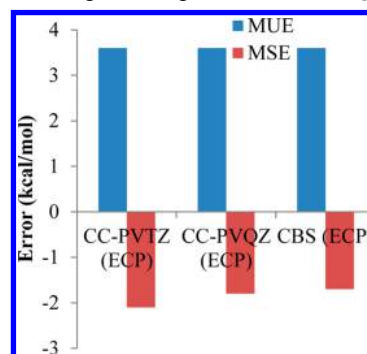


copper, the ECP results were selected. We remark that DKH all-electron calculations with CC-PVTZ(DKH) basis sets would lead to similar conclusions. Already at CC-PVTZ level the overall coinage metals MUE is 2.1 kcal/mol and the MSE is 0.4 kcal/mol. Upon increase of the basis set to CC-PVQZ quality the MUE does not change and the MSE becomes 0.2 kcal/mol, which is quite small. Finally, at CBS limit slightly higher MUE is obtained, namely 2.2 kcal/mol, while MSE gets smaller, namely -0.1 kcal/mol. It has to be noticed that the accuracy close to 2.1 kcal/mol has been obtained, and, which is very important, the calculations are essentially converged at the triple- $\zeta$  quality basis set. That means that DLPNO-CCSD(T)/CC-PVTZ calculations are already very accurate, and high quality CCSD(T) estimates can be obtained for very large molecules, since very time-consuming CC-PVQZ calculations could be avoided.

**3.4.2. M06.** Finally, in the light of the insightful discussion promoted by Xu et al. on whether practical CCSD(T) calculations agree better than DFT when compared to experimental data for dissociation energies of bonds to transition metals,<sup>76</sup> we decided to extend the current research with one representative DFT method, since the main scope of this work is not an extensive benchmark of DFT methods. Due to its excellent work in describing of transition metal–noncovalent ligand bond breaking,<sup>1,117,118</sup> we selected the M06 functional of Zhao et al.<sup>15,17</sup> for the evaluation of the

dissociation enthalpies of our data set. The errors obtained for all 72 dissociation reactions involving coinage metal ions are given in Chart 10. First, the overall MUE obtained for M06 is

**Chart 10.** M06/CC-PVNZ (ECP) Mean Unsigned (MUE) and Mean Signed (MSE) Errors with Respect to Experimental Values Obtained for All 72 Dissociation Enthalpies Involving  $\text{Cu}^+$ ,  $\text{Ag}^+$ , and  $\text{Au}^+$  Complexes



3.3 kcal/mol at CBS limit and the MSE is -1.7 kcal/mol. Considering that DFT methods are clearly faster than DLPNO-CCSD(T), the overall performance of the M06 functional is remarkable. Indeed, it results in a small tendency to overestimate the dissociation enthalpy relative to DLPNO-CCSD(T), resulting in negative MSEs. Finally, it has to be noticed that M06 dissociation enthalpies are essentially converged at the triple- $\zeta$  quality basis set. In this regard, our results can be regarded as another support to consider DFT as a reliable method for transition metals chemistry,<sup>76</sup> although it is clear that more functionals and other transition metals have to be considered in the tests.<sup>119,120</sup>

## 4. CONCLUSIONS

The recently developed DLPNO-CCSD(T) method was tested in reproducing 72 noncovalent ligand–transition metal ion ( $\text{Ag}^+$ ,  $\text{Cu}^+$ , and  $\text{Au}^+$ ) gas phase dissociation enthalpies measured experimentally. The best protocol we used, namely, DLPNO-CCSD(T)/CC-PVTZ(ECP) results in remarkable accuracy, with overall MUE 2.1 kcal/mol. All large deviations of our theoretical estimates from the experimentally documented values were explained. It was shown that the found deviations are not necessarily due to shortcomings of DLPNO-CCSD(T) scheme but could be attributed to quite large errors, documented or not, in the experimental enthalpies. Scalar relativistic effects turned out to be non-negligible for copper complexes, and their inclusion in the calculations either through relativistic ECP or through the Hamiltonian were proved to be fundamental, moreover, ECP and DKH based dissociation enthalpies turned out to be of the same quality for copper. Gratifying, results are converged already at the CC-PVTZ quality basis set, which allows to routinely obtain highly accurate DLPNO-CCSD(T) dissociation enthalpies for the transition metal complexes consisting of >100 atoms. The results encourage to apply DLPNO-CCSD(T) for single-point energy evaluations in calculations related to transition metal catalysis. However, since there is increasing evidence that for some specific problem in TM chemistry<sup>76</sup> and noncovalent interactions<sup>121</sup> the accuracy of CCSD(T) cannot be considered satisfactory, more tests involving other metal complex would be a good subject for the future study. Finally, overall good

performance is provided by the M06 functional, with MUE and MSE of 3.3 kcal/mol and  $-1.7$  kcal/mol.

## ■ ASSOCIATED CONTENT

### Supporting Information

The Supporting Information is available free of charge on the ACS Publications website at DOI: 10.1021/acs.jctc.5b00584.

Cartesian coordinates (Å), M06, DLPNO-CCSD(T), with different basis sets, T1 diagnostic values, enthalpic and ZPE corrections, tabulated enthalpies and errors forming the basis of charts (PDF)

## ■ AUTHOR INFORMATION

### Corresponding Author

\*E-mail: Luigi.Cavallo@kaust.edu.sa.

### Funding

This research has been supported by the King Abdullah University of Science and Technology, KAUST.

### Notes

The authors declare no competing financial interest.

## ■ REFERENCES

- (1) Cramer, C. J.; Truhlar, D. G. Density functional theory for transition metals and transition metal chemistry. *Phys. Chem. Chem. Phys.* **2009**, *11*, 10757–10816.
- (2) Sameera, W. M. C.; Maseras, F. Transition metal catalysis by density functional theory and density functional theory/molecular mechanics. *WIREs Comput. Mol. Sci.* **2012**, *2*, 375–385.
- (3) Thiel, W. Computational catalysis—past, present, and future. *Angew. Chem., Int. Ed.* **2014**, *53*, 8605–8613.
- (4) Jover, J.; Fey, N. The Computational Road to Better Catalysts. *Chem. - Asian J.* **2014**, *9*, 1714–1723.
- (5) Schlögl, R. Heterogeneous Catalysis. *Angew. Chem., Int. Ed.* **2015**, *54*, 3465–3520.
- (6) Cheng, G.-J.; Zhang, X.; Chung, L. W.; Xu, L.; Wu, Y.-D. Computational organic chemistry: bridging theory and experiment in establishing the mechanisms of chemical reactions. *J. Am. Chem. Soc.* **2015**, *137*, 1706–1725.
- (7) Jiménez-Hoyos, C. A.; Janesko, B. G.; Scuseria, G. E. Evaluation of range-separated hybrid and other density functional approaches on test sets relevant for transition metal-based homogeneous catalysts. *J. Phys. Chem. A* **2009**, *113*, 11742–11749.
- (8) Plata, R. E.; Singleton, D. A. A case study of the mechanism of alcohol-mediated Morita–Bailly–Hillman reactions. The importance of experimental observations. *J. Am. Chem. Soc.* **2015**, *137*, 3811–3826.
- (9) Harvey, J. N. On the accuracy of density functional theory in transition metal chemistry. *Annu. Rep. Prog. Chem., Sect. C: Phys. Chem.* **2006**, *102*, 203–226.
- (10) Cramer, C. J. *Essentials of Computational Chemistry: Theories and Models*, 2nd ed.; Wiley: West Sussex, U.K., 2005.
- (11) Jensen, F. *Introduction to Computational Chemistry*; 2nd ed.; Wiley: Chichester, U.K., 2006; p 620.
- (12) Koch, W.; Holthausen, M. C.; Baerends, E. J. *A Chemist's Guide to Density Functional Theory*; FVA-Frankfurter Verlagsanstalt GmbH: Weinheim, Germany, 2001.
- (13) Cohen, A. J.; Mori-Sánchez, P.; Yang, W. Challenges for Density Functional Theory. *Chem. Rev.* **2012**, *112*, 289–320.
- (14) Zhao, Y.; Truhlar, D. G. A new local density functional for main-group thermochemistry, transition metal bonding, thermochemical kinetics, and noncovalent interactions. *J. Chem. Phys.* **2006**, *125*, 194101.
- (15) Zhao, Y.; Truhlar, D. G. The M06 suite of density functionals for main group thermochemistry, thermochemical kinetics, non-covalent interactions, excited states, and transition elements: two new functionals and systematic testing of four M06-class functionals and 12 other functionals. *Theor. Chem. Acc.* **2008**, *120*, 215–241.
- (16) Schultz, N. E.; Zhao, Y.; Truhlar, D. G. Density functionals for inorganometallic and organometallic chemistry. *J. Phys. Chem. A* **2005**, *109*, 11127–11143.
- (17) Zhao, Y.; Schultz, N. E.; Truhlar, D. G. Design of density functionals by combining the method of constraint satisfaction with parametrization for thermochemistry, thermochemical kinetics, and noncovalent interactions. *J. Chem. Theory Comput.* **2006**, *2*, 364–382.
- (18) Geerlings, P.; De Proft, F.; Langenaeker, W. Conceptual density functional theory. *Chem. Rev.* **2003**, *103*, 1793–1873.
- (19) Kohn, W.; Becke, A. D.; Parr, R. G. Density functional theory of electronic structure. *J. Phys. Chem.* **1996**, *100*, 12974–12980.
- (20) Parr, R. G.; Yang, W. T. Density functional theory of the electronic structure of molecules. *Annu. Rev. Phys. Chem.* **1995**, *46*, 701–728.
- (21) Baerends, E. J.; Gritsenko, O. V. A quantum chemical view of density functional theory. *J. Phys. Chem. A* **1997**, *101*, 5383–5403.
- (22) Grimme, S. Density functional theory with London dispersion corrections. *WIREs Comput. Mol. Sci.* **2011**, *1*, 211–228.
- (23) Chermak, E.; Mussard, B.; Angyan, J. G.; Reinhardt, P. Short range DFT combined with long-range local RPA within a range-separated hybrid DFT framework. *Chem. Phys. Lett.* **2012**, *550*, 162–169.
- (24) Garza, A. J.; Jiménez-Hoyos, C. A.; Scuseria, G. E. Capturing static and dynamic correlations by a combination of projected Hartree-Fock and density functional theories. *J. Chem. Phys.* **2013**, *138*, 134102.
- (25) Haunschild, R.; Scuseria, G. E. Range-separated local hybrids. *J. Chem. Phys.* **2010**, *132*, 224106.
- (26) Haunschild, R.; Henderson, T. M.; Jimenez-Hoyos, C. A.; Scuseria, G. E. Many-electron self-interaction and spin polarization errors in local hybrid density functionals. *J. Chem. Phys.* **2010**, *133*, 134116.
- (27) Janesko, B. G.; Henderson, T. M.; Scuseria, G. E. Screened hybrid density functionals for solid-state chemistry and physics. *Phys. Chem. Chem. Phys.* **2009**, *11*, 443–454.
- (28) Szabo, A.; Ostlund, N. S. *Modern Quantum Chemistry: Introduction to Advanced Electronic Structure Theory*; Courier Corporation: New York, 2012.
- (29) Hättig, C.; Weigend, F. CC2 excitation energy calculations on large molecules using the resolution of the identity approximation. *J. Chem. Phys.* **2000**, *113*, 5154–5161.
- (30) Neese, F.; Wennmohs, F.; Hansen, A. Efficient and accurate local approximations to coupled-electron pair approaches: An attempt to revive the pair natural orbital method. *J. Chem. Phys.* **2009**, *130*, 114108.
- (31) Werner, H.-J.; Schütz, M. An efficient local coupled cluster method for accurate thermochemistry of large systems. *J. Chem. Phys.* **2011**, *135*, 144116.
- (32) Liakos, D. G.; Hansen, A.; Neese, F. Weak Molecular Interactions Studied with Parallel Implementations of the Local Pair Natural Orbital Coupled Pair and Coupled Cluster Methods. *J. Chem. Theory Comput.* **2011**, *7*, 76–87.
- (33) Boughton, J. W.; Pulay, P. Comparison of the boys and Pipek-Mezey localizations in the local correlation approach and automatic virtual basis selection. *J. Comput. Chem.* **1993**, *14*, 736–740.
- (34) Riplinger, C.; Neese, F. An efficient and near linear scaling pair natural orbital based local coupled cluster method. *J. Chem. Phys.* **2013**, *138*, 034106.
- (35) Riplinger, C.; Sandhoefer, B.; Hansen, A.; Neese, F. Natural triple excitations in local coupled cluster calculations with pair natural orbitals. *J. Chem. Phys.* **2013**, *139*, 134101.
- (36) Ayala, P. Y.; Scuseria, G. E. Linear scaling second-order Møller-Plesset theory in the atomic orbital basis for large molecular systems. *J. Chem. Phys.* **1999**, *110*, 3660–3671.
- (37) Saebo, S.; Pulay, P. Local treatment of electron correlation. *Annu. Rev. Phys. Chem.* **1993**, *44*, 213–236.
- (38) Hampel, C.; Werner, H. J. Local treatment of electron correlation in coupled cluster theory. *J. Chem. Phys.* **1996**, *104*, 6286–6297.

- (39) Schütz, M.; Werner, H. J. Local perturbative triples correction (T) with linear cost scaling. *Chem. Phys. Lett.* **2000**, *318*, 370–378.
- (40) Liakos, D. G.; Sparta, M.; Kesharwani, M. K.; Martin, J. M. L.; Neese, F. Exploring the Accuracy Limits of Local Pair Natural Orbital Coupled-Cluster Theory. *J. Chem. Theory Comput.* **2015**, *11*, 1525–1539.
- (41) Edmiston, C.; Krauss, M. Pseudonatural orbitals as a basis for superposition of configurations. *J. Chem. Phys.* **1966**, *45*, 1833.
- (42) Sparta, M.; Neese, F. Chemical applications carried out by local pair natural orbital based coupled-cluster methods. *Chem. Soc. Rev.* **2014**, *43*, S032–S041.
- (43) Friedrich, J.; Haenchen, J. Incremental CCSD(T)(F12\*) vertical bar IMP2: a black box method to obtain highly accurate reaction energies. *J. Chem. Theory Comput.* **2013**, *9*, 5381–5394.
- (44) Liakos, D. G.; Neese, F. Interplay of Correlation and Relativistic Effects in Correlated Calculations on Transition-Metal Complexes: The  $(\text{Cu}_2\text{O}_2)^{2+}$  Core Revisited. *J. Chem. Theory Comput.* **2011**, *7*, 1511–1523.
- (45) Riplinger, C.; Sampson, M. D.; Ritzmann, A. M.; Kubiak, C. P.; Carter, E. A. Mechanistic Contrasts between Manganese and Rhenium Bipyridine Electrocatalysts for the Reduction of Carbon Dioxide. *J. Am. Chem. Soc.* **2014**, *136*, 16285–16298.
- (46) Sparta, M.; Riplinger, C.; Neese, F. Mechanism of Olefin Asymmetric Hydrogenation Catalyzed by Iridium Phosphino-Oxazoline: A Pair Natural Orbital Coupled Cluster Study. *J. Chem. Theory Comput.* **2014**, *10*, 1099–1108.
- (47) Hansen, A.; Bannwarth, C.; Grimme, S.; Petrovic, P.; Werle, C.; Djukic, J.-P. The Thermochemistry of London Dispersion-Driven Transition Metal Reactions: Getting the 'Right Answer for the Right Reason'. *ChemistryOpen* **2014**, *3*, 177–189.
- (48) Maganas, D.; Roemelt, M.; Haevecker, M.; Trunschke, A.; Knop-Gericke, A.; Schloegl, R.; Neese, F. First principles calculations of the structure and V L-edge X-ray absorption spectra of  $\text{V}_2\text{O}_5$  using local pair natural orbital coupled cluster theory and spin-orbit coupled configuration interaction approaches. *Phys. Chem. Chem. Phys.* **2013**, *15*, 7260–7276.
- (49) Neese, F. The ORCA program system. *WIREs Comput. Mol. Sci.* **2012**, *2*, 73–78.
- (50) Perdew, J. P.; Burke, K.; Ernzerhof, M. Generalized gradient approximation made simple. *Phys. Rev. Lett.* **1996**, *77*, 3865–3868.
- (51) Perdew, J. P.; Burke, K.; Ernzerhof, M. Generalized gradient approximation made simple (vol 77, pg 3865, 1996). *Phys. Rev. Lett.* **1997**, *78*, 1396–1396.
- (52) Grimme, S.; Antony, J.; Ehrlich, S.; Krieg, H. A consistent and accurate ab initio parametrization of density functional dispersion correction (DFT-D) for the 94 elements H-Pu. *J. Chem. Phys.* **2010**, *132*, 154104.
- (53) Minenkov, Y.; Singstad, Å.; Occhipinti, G.; Jensen, V. R. The accuracy of DFT-optimized geometries of functional transition metal compounds: a validation study of catalysts for olefin metathesis and other reactions in the homogeneous phase. *Dalton Transactions* **2012**, *41*, 5526–5541.
- (54) Hujo, W.; Grimme, S. Performance of Non-Local and Atom-Pairwise Dispersion Corrections to DFT for Structural Parameters of Molecules with Noncovalent Interactions. *J. Chem. Theory Comput.* **2013**, *9*, 308–315.
- (55) Pandey, K. K.; Patidar, P.; Bariya, P. K.; Patidar, S. K.; Vishwakarma, R. Assessment of density functionals and paucity of non-covalent interactions in aminopyrene complexes of molybdenum and tungsten  $[(\eta^5\text{-C}_5\text{H}_5)(\text{CO})_2\text{EN}(\text{SiMe}_3)(\text{R})]$  (E = Si, Ge, Sn, Pb): a dispersion-corrected DFT study. *Dalton Transactions* **2014**, *43*, 9955–9967.
- (56) Weigend, F.; Ahlrichs, R. Balanced basis sets of split valence, triple zeta valence and quadruple zeta valence quality for H to Rn: Design and assessment of accuracy. *Phys. Chem. Chem. Phys.* **2005**, *7*, 3297–3305.
- (57) Weigend, F. Accurate Coulomb-fitting basis sets for H to Rn. *Phys. Chem. Chem. Phys.* **2006**, *8*, 1057–1065.
- (58) Andrae, D.; Häussermann, U.; Dolg, M.; Stoll, H.; Preuss, H. Energy-adjusted abinitio pseudopotentials for the 2nd and 3rd row transition elements. *Theor. Chim. Acta* **1990**, *77*, 123–141.
- (59) Figgen, D.; Rauhut, G.; Dolg, M.; Stoll, H. Energy-consistent pseudopotentials for group 11 and 12 atoms: adjustment to multi-configuration Dirac-Hartree-Fock data. *Chem. Phys.* **2005**, *311*, 227–244.
- (60) Peterson, K. A.; Puzarini, C. Systematically convergent basis sets for transition metals. II. Pseudopotential-based correlation consistent basis sets for the group 11 (Cu, Ag, Au) and 12 (Zn, Cd, Hg) elements. *Theor. Chem. Acc.* **2005**, *114*, 283–296.
- (61) Dunning, T. H. Gaussian-basis sets for use in correlated molecular calculations 0.1. The atoms boron through neon and hydrogen. *J. Chem. Phys.* **1989**, *90*, 1007–1023.
- (62) Woon, D. E.; Dunning, T. H. Gaussian-Basis Sets for use in Correlated Molecular Calculations 0.3. The Atoms Aluminum through Argon. *J. Chem. Phys.* **1993**, *98*, 1358–1371.
- (63) Woon, D. E.; Dunning, T. H. Gaussian-basis sets for use in correlated molecular calculations 0.5. Core-valence basis-sets for boron through neon. *J. Chem. Phys.* **1995**, *103*, 4572–4585.
- (64) Weigend, F.; Kohn, A.; Hattig, C. Efficient use of the correlation consistent basis sets in resolution of the identity MP2 calculations. *J. Chem. Phys.* **2002**, *116*, 3175–3183.
- (65) Balabanov, N. B.; Peterson, K. A. Systematically convergent basis sets for transition metals. I. All-electron correlation consistent basis sets for the 3d elements Sc-Zn. *J. Chem. Phys.* **2005**, *123*, 064107.
- (66) Reiher, M.; Wolf, A. Exact decoupling of the Dirac Hamiltonian. II. The generalized Douglas-Kroll-Hess transformation up to arbitrary order. *J. Chem. Phys.* **2004**, *121*, 10945–10956.
- (67) Pantazis, D. A.; Chen, X.-Y.; Landis, C. R.; Neese, F. All-electron scalar relativistic basis sets for third-row transition metal atoms. *J. Chem. Theory Comput.* **2008**, *4*, 908–919.
- (68) Halkier, A.; Helgaker, T.; Jørgensen, P.; Klopper, W.; Koch, H.; Olsen, J.; Wilson, A. K. Basis-set convergence in correlated calculations on Ne, N-2, and H2O. *Chem. Phys. Lett.* **1998**, *286*, 243–252.
- (69) Helgaker, T.; Klopper, W.; Koch, H.; Noga, J. Basis-set convergence of correlated calculations on water. *J. Chem. Phys.* **1997**, *106*, 9639–9646.
- (70) Halkier, A.; Helgaker, T.; Jørgensen, P.; Klopper, W.; Olsen, J. Basis-set convergence of the energy in molecular Hartree-Fock calculations. *Chem. Phys. Lett.* **1999**, *302*, 437–446.
- (71) Boys, S. F.; Bernardi, F. Calculation of small molecular interactions by differences of separate total energies - some procedures with reduced errors. *Mol. Phys.* **1970**, *19*, 553–559.
- (72) Burns, L. A.; Marshall, M. S.; Sherrill, C. D. Comparing Counterpoise-Corrected, Uncorrected, and Averaged Binding Energies for Benchmarking Noncovalent Interactions. *J. Chem. Theory Comput.* **2014**, *10*, 49–57.
- (73) Alvarez-Idaboy, J. R.; Galano, A. Counterpoise corrected interaction energies are not systematically better than uncorrected ones: comparison with CCSD(T) CBS extrapolated values. *Theor. Chem. Acc.* **2010**, *126*, 75–85.
- (74) Francisco-Márquez, M.; Alvarez-Idaboy, J. R.; Galano, A.; Vivier-Bunge, A. Quantum chemistry and TST study of the mechanism and kinetics of the butadiene and isoprene reactions with mercapto radicals. *Chem. Phys.* **2008**, *344*, 273–280.
- (75) Gruber-Stadler, M.; Muehlhaeuser, M.; Sellevag, S. R.; Nielsen, C. J. A quantum chemistry study of the Cl atom reaction with formaldehyde. *J. Phys. Chem. A* **2008**, *112*, 9–22.
- (76) Xu, X.; Zhang, W.; Tang, M.; Truhlar, D. G. Do Practical Standard Coupled Cluster Calculations Agree Better than Kohn-Sham Calculations with Currently Available Functionals When Compared to the Best Available Experimental Data for Dissociation Energies of Bonds to 3d Transition Metals? *J. Chem. Theory Comput.* **2015**, *11*, 2036–2052.
- (77) Holland, P. M.; Castleman, A. W. The thermochemical properties of gas-phase transition-metal ion complexes. *J. Chem. Phys.* **1982**, *76*, 4195–4205.



- (78) Guo, B. C.; Castleman, A. W. The bonding strength of  $\text{Ag}^+(\text{C}_2\text{H}_4)$  and  $\text{Ag}^+(\text{C}_2\text{H}_4)_2$  complexes. *Chem. Phys. Lett.* **1991**, *181*, 16–20.
- (79) Manard, M. J.; Kemper, P. R.; Bowers, M. T. Binding interactions of mono- and diatomic silver cations with small alkenes: experiment and theory. *Int. J. Mass Spectrom.* **2005**, *241*, 109–117.
- (80) Meyer, F.; Chen, Y. M.; Armentrout, P. B. Sequential bond-energies of  $\text{Cu}(\text{CO})_x^+$  and  $\text{Ag}(\text{CO})_x^+$  ( $x = 1-4$ ). *J. Am. Chem. Soc.* **1995**, *117*, 4071–4081.
- (81) Ho, Y. P.; Yang, Y. C.; Klippenstein, S. J.; Dunbar, R. C. Binding energies of  $\text{Ag}^+$  and  $\text{Cd}^+$  complexes from analysis of radiative association kinetics. *J. Phys. Chem. A* **1997**, *101*, 3338–3347.
- (82) Shoeib, T.; El Aribi, H.; Siu, K. W. M.; Hopkinson, A. C. A study of silver (I) ion-organonitrile complexes: Ion structures, binding energies, and substituent effects. *J. Phys. Chem. A* **2001**, *105*, 710–719.
- (83) El Aribi, H.; Shoeib, T.; Ling, Y.; Rodriguez, C. F.; Hopkinson, A. C.; Siu, K. W. M. Binding energies of the silver ion to small oxygen-containing ligands: Determination by means of density functional theory and threshold collision-induced dissociation. *J. Phys. Chem. A* **2002**, *106*, 2908–2914.
- (84) Rodgers, M. T.; Armentrout, P. B. Noncovalent metal-ligand bond energies as studied by threshold collision-induced dissociation. *Mass Spectrom. Rev.* **2000**, *19*, 215–247.
- (85) Magnera, T. F.; David, D. E.; Stulik, D.; Orth, R. G.; Jonkman, H. T.; Michl, J. Production of hydrated metal-ions by fast ion or atom beam sputtering - collision-induced dissociation and successive hydration energies of gaseous  $\text{Cu}^+$  with 1–4 water-molecules. *J. Am. Chem. Soc.* **1989**, *111*, 5036–5043.
- (86) Dalleska, N. F.; Honma, K.; Sunderlin, L. S.; Armentrout, P. B. Solvation of transition-metal ions by water - sequential binding-energies of  $\text{M}^+(\text{H}_2\text{O})_x$  ( $x = 1-4$ ) for  $\text{M} = \text{Ti}$  to  $\text{Cu}$  determined by collision-induced dissociation. *J. Am. Chem. Soc.* **1994**, *116*, 3519–3528.
- (87) Chu, Y.; Yang, Z.; Rodgers, M. T. Solvation of copper ions by acetone. Structures and sequential binding energies of  $\text{Cu}^+(\text{acetone})_x$   $x = 1-4$  from collision-induced dissociation and theoretical studies. *J. Am. Soc. Mass Spectrom.* **2002**, *13*, 453–468.
- (88) Walter, D.; Armentrout, P. B. Sequential bond dissociation energies of  $\text{M}^+(\text{NH}_3)_x$  ( $x = 1-4$ ) for  $\text{M} = \text{Ti}-\text{Cu}$ . *J. Am. Chem. Soc.* **1998**, *120*, 3176–3187.
- (89) Bauschlicher, C. W.; Langhoff, S. R.; Partridge, H. The binding-energies of  $\text{Cu}^+(\text{H}_2\text{O})_n$  and  $\text{Cu}^+(\text{NH}_3)_n$  ( $n = 1-4$ ). *J. Chem. Phys.* **1991**, *94*, 2068–2072.
- (90) Meyer, F.; Khan, F. A.; Armentrout, P. B. Thermochemistry of transition-metal benzene complexes - binding-energies of  $\text{M}(\text{C}_6\text{H}_6)_x^+$  ( $x = 1, 2$ ) for  $\text{M} = \text{Ti}$  to  $\text{Cu}$ . *J. Am. Chem. Soc.* **1995**, *117*, 9740–9748.
- (91) Langhoff, S. R.; Bauschlicher, C. W.; Partridge, H.; Sodupe, M. Theoretical-study of one and 2-ammonia molecules bound to the 1st-row transition-metal ions. *J. Phys. Chem.* **1991**, *95*, 10677–10681.
- (92) Koizumi, H.; Zhang, X. G.; Armentrout, P. B. Collision-induced dissociation and theoretical studies of  $\text{Cu}^+$ -dimethyl ether complexes. *J. Phys. Chem. A* **2001**, *105*, 2444–2452.
- (93) Sievers, M. R.; Jarvis, L. M.; Armentrout, P. B. Transition-metal ethene bonds: Thermochemistry of  $\text{M}^+(\text{C}_2\text{H}_4)_n$  ( $\text{M} = \text{Ti}-\text{Cu}$ ,  $n = 1$  and 2) complexes. *J. Am. Chem. Soc.* **1998**, *120*, 1891–1899.
- (94) Vitale, G.; Valina, A. B.; Huang, H.; Amunugama, R.; Rodgers, M. T. Solvation of copper ions by acetonitrile. Structures and sequential binding energies of  $\text{Cu}^+(\text{CH}_3\text{CN})_x$   $x = 1-5$ , from collision-induced dissociation and theoretical studies. *J. Phys. Chem. A* **2001**, *105*, 11351–11364.
- (95) Gapeev, A.; Yang, C. N.; Klippenstein, S. J.; Dunbar, R. C. Binding energies of gas-phase metal ions with pyrrole: Experimental and quantum chemical results. *J. Phys. Chem. A* **2000**, *104*, 3246–3256.
- (96) Rodgers, M. T.; Stanley, J. R.; Amunugama, R. Periodic trends in the binding of metal ions to pyridine studied by threshold collision-induced dissociation and density functional theory. *J. Am. Chem. Soc.* **2000**, *122*, 10969–10978.
- (97) Amunugama, R.; Rodgers, M. T. Periodic trends in the binding of metal ions to pyrimidine studied by threshold collision-induced dissociation and density functional theory. *J. Phys. Chem. A* **2001**, *105*, 9883–9892.
- (98) Rodgers, M. T.; Armentrout, P. B. Influence of d orbital occupation on the binding of metal ions to adenine. *J. Am. Chem. Soc.* **2002**, *124*, 2678–2691.
- (99) Jašíková, L.; Roithová, J. Interaction of the Gold(I) Cation  $\text{Au}(\text{PMe}_3)^+$  with Unsaturated Hydrocarbons. *Organometallics* **2012**, *31*, 1935–1942.
- (100) Schwarz, H. Relativistic effects in gas-phase ion chemistry: An experimentalist's view. *Angew. Chem., Int. Ed.* **2003**, *42*, 4442–4454.
- (101) Poisson, L.; Lepetit, F.; Mestdag, J. M.; Visticot, J. P. Multifragmentation of the  $\text{Au}(\text{H}_2\text{O})_{n \leq 10}^+$  cluster ions by collision with helium. *J. Phys. Chem. A* **2002**, *106*, 5455–5462.
- (102) Ho, Y. P.; Dunbar, R. C. Reactions of  $\text{Au}^+$  and  $\text{Au}^-$  with benzene and fluorine-substituted benzenes. *Int. J. Mass Spectrom.* **1999**, *182*, 175–184.
- (103) Deng, H. T.; Kebarle, P. Binding energies of silver ion ligand,  $\text{L}$ , complexes  $\text{AgL}_2^+$  determined from ligand-exchange equilibria in the gas phase. *J. Phys. Chem. A* **1998**, *102*, 571–579.
- (104) Fox, B. S.; Beyer, M. K.; Bondybey, V. E. Coordination chemistry of silver cations. *J. Am. Chem. Soc.* **2002**, *124*, 13613–13623.
- (105) Widmer-Cooper, A. N.; Lindoy, L. F.; Reimers, J. R. The effect of alkylation of N- and O-donor atoms on their strength of coordination to silver(I). *J. Phys. Chem. A* **2001**, *105*, 6567–6574.
- (106) Wood, J. H.; Boring, A. M. Improved Pauli Hamiltonian for local-potential problems. *Phys. Rev. B: Condens. Matter Mater. Phys.* **1978**, *18*, 2701–2711.
- (107) Antes, I.; Frenking, G. Structure and bonding of the transition-metal methyl and phenyl compounds  $\text{MCH}_3$  and  $\text{MC}_6\text{H}_5$  ( $\text{M} = \text{Cu}$ ,  $\text{Ag}$ ,  $\text{Au}$ ) and  $\text{M}(\text{CH}_3)_2$  and  $\text{M}(\text{C}_6\text{H}_5)_2$  ( $\text{M} = \text{Zn}$ ,  $\text{Cd}$ ,  $\text{Hg}$ ). *Organometallics* **1995**, *14*, 4263–4268.
- (108) Desclaux, J. P.; Pyykkö, P. Dirac-Fock one-center calculations - molecules  $\text{CuH}$ ,  $\text{AgH}$  and  $\text{AuH}$  including p-type symmetry functions. *Chem. Phys. Lett.* **1976**, *39*, 300–303.
- (109) Pyykkö, P. Relativistic effects in structural chemistry. *Chem. Rev.* **1988**, *88*, 563–594.
- (110) Dolg, M. Relativistic effective core potentials. *Theor. Comput. Chem.* **2002**, *11*, 793–862.
- (111) Matito, E.; Salvador, P.; Styszynski, J. Benchmark calculations of metal carbonyl cations: relativistic vs. electron correlation effects. *Phys. Chem. Chem. Phys.* **2013**, *15*, 20080–20090.
- (112) Lupinetti, A. J.; Jonas, V.; Thiel, W.; Strauss, S. H.; Frenking, G. Trends in molecular geometries and bond strengths of the homoleptic d(10) metal carbonyl cations  $\text{M}(\text{CO})_n^{x+}$  ( $\text{M}^+ = \text{Cu}^+$ ,  $\text{Ag}^+$ ,  $\text{Au}^+$ ,  $\text{Zn}^{2+}$ ,  $\text{Cd}^{2+}$ ,  $\text{Hg}^{2+}$ ;  $n = 1-6$ ): A theoretical study. *Chem. - Eur. J.* **1999**, *5*, 2573–2583.
- (113) Yang, Y. S.; Hsu, W. Y.; Lee, H. F.; Huang, Y. C.; Yeh, C. S.; Hu, C. H. Experimental and theoretical studies of metal cation-pyridine complexes containing  $\text{Cu}$  and  $\text{Ag}$ . *J. Phys. Chem. A* **1999**, *103*, 11287–11292.
- (114) Velasquez, J., III; Njagic, B.; Gordon, M. S.; Duncan, M. A. IR photodissociation spectroscopy and theory of  $\text{Au}^+(\text{CO})_n$  complexes: Nonclassical carbonyls in the gas phase. *J. Phys. Chem. A* **2008**, *112*, 1907–1913.
- (115) Hrusák, J.; Hertwig, R. H.; Schröder, D.; Schwerdtfeger, P.; Koch, W.; Schwarz, H. Relativistic effects in cationic gold(i) complexes - a comparative-study of ab-initio pseudopotential and density-functional methods. *Organometallics* **1995**, *14*, 1284–1291.
- (116) Lee, H. M.; Min, S. K.; Lee, E. C.; Min, J. H.; Odde, S.; Kim, K. S. Hydrated copper and gold monovalent cations: Ab initio study. *J. Chem. Phys.* **2005**, *122*, 064314.
- (117) Poater, A.; Pump, E.; Vummaleti, S. V. C.; Cavallo, L. The Right Computational Recipe for Olefin Metathesis with Ru-Based Catalysts: The Whole Mechanism of Ring-Closing Olefin Metathesis. *J. Chem. Theory Comput.* **2014**, *10*, 4442–4448.
- (118) Minenkov, Y.; Occhipinti, G.; Jensen, V. R. Metal-Phosphine Bond Strengths of the Transition Metals: A Challenge for DFT. *J. Phys. Chem. A* **2009**, *113*, 11833–11844.

(119) Fröhlich, N.; Frenking, G., Theoretical prediction of bond dissociation energies for transition metal compounds and main group complexes with standard quantum-chemical methods. In *Quantum-Mechanical Prediction of Thermochemical Data*; Cioslowski, J., Ed.; Springer: Netherlands, 2001; Vol. 22, pp 199–233.

(120) Diedenhofen, M.; Wagener, T.; Frenking, G., The accuracy of quantum chemical methods for the calculation of transition metal compounds. In *Computational Organometallic Chemistry*, 1 ed.; Cundari, T. R., Ed.; CRC Press: Boca Raton, FL, 2001; pp 69–121.

(121) Řezáč, J.; Hobza, P. Describing Noncovalent Interactions beyond the Common Approximations: How Accurate Is the "Gold Standard," CCSD(T) at the Complete Basis Set Limit? *J. Chem. Theory Comput.* **2013**, 9, 2151–2155.

#### ■ NOTE ADDED AFTER ASAP PUBLICATION

An uncorrected version posted ASAP September 4, 2015, the correct version reposted later on September 4, 2015.